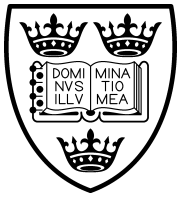
Modelling Rainforests



Caroline Bampfylde

St Cross College

University of Oxford

A dissertation submitted in partial fulfilment for the degree of

Master of Science
Mathematical Modelling & Numerical Analysis

Trinity 1999

This dissertation is dedicated to
My Parents and Richard, Christopher and René
for being interested but never really quite understanding!

Acknowledgements

To start with I would like to thank the botany team on the BSES Queensland expedition (1995). To live and work in the rainforest with you was fantastic. Who would have thought it would have led this far?

Next my supervisors, David Gavaghan, Philip Maini & Nick Brown for all your patience, support and advice throughout the project.

All the MSc. for providing general entertainment and amusement and in particular Déirdre, café partner, and Liam, fellow G17 mate.

The Comlab for having my matrix up on most of the whiteboards.

Keith Gillow, for answering my numerous LaTeX queries and resolving my memory problems.

The Engineering and Physical Sciences Research Council for their financial support.

Finally St. Cross for providing me with such great lunches, so conveniently located.

Abstract

In this dissertation, we develop a competition-colonisation model to describe the dynamics of interactions between tropical rainforest tree species.

There is a great deal of interest in modelling rainforest diversity. Understanding the natural processes that maintain diversity is essential so that sustainable management systems can attempt to replicate important processes.

We find, through numerical investigation and analysis, that with constant colonisation rates, c_i, we cannot predict multiple species coexistence. The inclusion of decaying colonisation rates, describing the seedling population decay over time, and random mass fruiting events allows coexistence of species, but using unrealistic parameter values. Finally we investigate a mathematical model without any competition between species and find that, using realistic parameter values, our results qualitatively mimic observations of rainforest dynamics. The results of the no competition model support Hubbell's null hypothesis [17].

Contents

1 Introduction **1**

1.1 Problem Description 1

1.2 Field Work Experiments and Observations 2

2 Literature review of the methods which may be applicable to modelling diversity and competition in tropical rainforests **5**

2.1 Introduction 5

2.2 Deterministic models 5

2.2.1 Tilman: spatial theory 6

2.2.1.1 Single species dynamics 6

2.2.1.2 Competition between two species 7

2.2.1.3 Multiple species competition 7

2.2.2 Habitat destruction 8

2.2.3 Imperfect trade-offs 8

2.3 Probabilistic approach 9

2.3.1 Recruitment limitation 9

2.3.2 Effects of competitive asymmetry 10

2.3.3 High species richness 11

2.3.4 Competition-colonisation model including niche hypothesis mechanism 11

2.3.5 Sexual reproduction 11

2.4 Other Models 12

2.4.1 Spatially explicit models 12

2.4.2 Age structured models 13

2.4.3 Dynamical systems approach to ecosystems 14

2.4.4 Virus dynamics 14

2.4.5 Population dynamics of insects 16

2.5 Conclusion 17

3 Two Species Model **18**
3.1 Introduction . . . 18
3.2 Model and Determination of Steady States . . . 18
3.3 Linear Stability Analysis . . . 20
3.4 Feasibility & Stability of Steady States . . . 21
3.5 Phase Plane Analysis . . . 22
3.6 Conclusion . . . 23

4 Three Species Model **27**
4.1 Introduction . . . 27
4.2 Model and Determination of Steady States . . . 27
4.3 Preliminary Analysis . . . 29
4.4 Numerical Experiments . . . 30
4.5 Further Stability Analysis . . . 31
4.6 Conclusion . . . 33

5 n-Species Model **34**
5.1 Introduction . . . 34
5.2 Model and Determination of Steady States . . . 34
5.3 Stability Analysis . . . 35
5.4 Conclusion . . . 36

6 Fruiting Events **37**
6.1 Motivation for Model . . . 37
6.2 Description of Model . . . 37
6.2.1 Colonisation Rates . . . 37
6.2.2 Model Dynamics Equations . . . 38
6.3 Problems with determination of parameter values . . . 38
6.4 Numerical Experiments . . . 39
6.5 Potential Adaptation to Model . . . 42
6.6 Conclusion . . . 43

7 No Competition **47**
7.1 Description of Model . . . 47
7.2 Conclusion . . . 48

8 Conclusion **49**
8.1 Plausibility of Hypothesis 49
8.2 Areas of Further Work 49

A Parameter Definitions **ai**

B Eigenvalues for Three Species Model **aii**

C Derivation of Parameters **aiv**
C.1 Decay Rates (β_i) . . . . . aiv
C.2 Colonisation Rates (α_i) . . . . . aiv
C.3 Mortality Rates (m_i) . . . . . av
C.4 Initial Proportional Abundances . . . . . av
C.5 Ratios of Mortality to Colonisation . . . . . avi
C.6 Fruiting Interval Length and Distribution . . . . . avi
C.7 Balance of Proliferation and Death of Species . . . . . avi

Bibliography **aviii**

List of Figures

1.1 Seedlings on the forest floor, Borneo 2
1.2 Forest canopy, Borneo 3
1.3 Idealised cross section of the rainforest 4

3.1 Plot of $\hat{\lambda_1}$ and $\hat{\lambda_2}$ showing the sign of the real part of the eigenvalues, cyan for $\mathbb{R}(\hat{\lambda_i}) \geq 0$, and white for $\mathbb{R}(\hat{\lambda_i}) < 0$ within the feasibility region (black lines show the boundaries). 22
3.2 Stability & feasibility regions, see text for details 23
3.3 Nullclines & steady states for different regions within the parameter plane (γ_1, γ_2) 24
3.4 Phase planes in the different regions of the parameter space (γ_1, γ_2). The top left hand panel corresponds to region 1 and follow the same order as Figure (3.3). 26

4.1 Feasibility regions for steady state (h) in the (γ_i, γ_j) planes 29
4.2 Feasibility regions for steady state (h) extended into the full 3-D parameter space 30
4.3 Phase planes and phase space for equations (4.6) - (4.8) for parameter values $\gamma_1 = 0.2$, $\gamma_2 = 0.1$, $\gamma_3 = 0.05$ 31
4.4 Phase planes and phase space for equations (4.6) - (4.8) for parameter values $\gamma_1 = 0.5$, $\gamma_2 = 0.4$, $\gamma_3 = 0.3$, initial conditions: $(p_1, p_2, p_3) = (0.200, 0.200, 0.100)$ 33

6.1 Dynamics of competition, equation (6.2) - (6.4) between 6 species. The top panel includes fruiting and decaying c_i, while the bottom panel shows that the simulation run without fruiting events and constant c_i results in one species dominating, after less than 150 years. 40
6.2 Dynamics of competition between 2 species, for the model (6.2) - (6.4), in sub-plot(1), both species are present after 350 years, but in sub-plots (2) and (3) one species is seen to dominate the other 41

6.3 Dynamics of competition between 4 species, for the model (6.2) - (6.4), in sub-plot(1), all species are present after 350 years, but in sub-plots (2), (3) and (4) one or more of the species are seen to start to die out. 43
6.4 Dynamics of competition between 180 species, for the model (6.2) - (6.4). See text for details. 44
6.5 Dynamics of competition between 180 species, for the model (6.2) - (6.4), showing that all species are present after 700 years 45
6.6 Dynamics of competition between 2 species, with an adaptation of the model to (6.6) 46

7.1 Dynamics of competition between 6 species, with no competition. 48

C.1 Time course of seedlings on forest floor . . . . . av

Chapter 1

Introduction

1.1 Problem Description

Rainforests are found in areas of high precipitation and typically contain a vast array of plant and animal life. The best known and the most ecologically diverse are the tropical rainforests of Asia and South America. The structure of a rainforest is different from that of a temperate forest. The top level is the canopy, formed by the crowns of the adult trees. Below this level (the understorey) are a lot of younger trees and saplings living in the shade of the canopy, waiting for an adult tree to die and fall to create a gap in the canopy. Once a gap has been formed, the saplings present will compete (for the available light) to fill the space and establish themselves. At the bottom of the forest is the forest floor, where seedlings of adult tree species are found together with decomposing matter from fallen leaves and trees. The photographs below (Figures (1.1) and (1.2)) show an example of a seedling on the forest floor and a view of the canopy from above. A sketch of a cross section of an (idealised) rainforest is also shown in Figure (1.3).

The diversity of tree species in the tropical rainforest is enormous and poses an important ecological problem. In any one hectare in Borneo there is likely to be about 180 different species, whilst in the adjoining hectare, a further 150 different species may be found. These figures must be compared to the figures for the UK, where there are only 38 native species in total. Very high plant species diversity is difficult to explain as the ecological range amongst green plants is rather small. Different animals eat different plants (or each other), but plants all need water, light and a very limited number of nutrients. Why is it that the species that are superior competitors for these resources are not necessarily the ones that dominate the tropical rainforest? Experiments have shown that both differences in plant structure and the plant's requirements for different resource concentrations can lead to an increase in the use of the resource base in any environment as species diversity increases.



Figure 1.1: Seedlings on the forest floor, Borneo

However, this increase in exploitation efficiency declines once there are greater than ten or more species. Beyond this number, most species appear to be functionally redundant.

There is a great deal of interest in modelling diversity. Understanding the natural processes that maintain diversity is important so that sustainable management systems can attempt to replicate important processes. The forest may need management if, for example, logging is taking place, or the forest needs to be regenerated after an oil spillage or other disaster.

Our main aim in this dissertation is to model the diversity and competition between different Dipterocarpaceae species in tropical rainforests, in an attempt to gain some insight into the mechanisms which allow so many species to co-exist (in Borneo there are 267 different Dipterocarpaceae species). In particular we wish to build a mathematical model which will allow us to investigate the validity of a hypothesis put forward by Dr. Nick Brown of the Department of Plant Sciences, described in the next section.

1.2 Field Work Experiments and Observations

Brown *et al* (1999) [5] have carried out growth experiments on natural populations of Dipterocarpaceae species of contrasting ecology growing in artificial gaps and the for-



Figure 1.2: Forest canopy, Borneo

est understorey. We shall concentrate our model on these species. Brown *et al*'s studies demonstrated that although differences exist between species in photosynthetic and growth responses to the high light environment, competition for light in canopy gaps is highly asymmetric and tends to reinforce any pre-existing dominance hierarchy (that is, all things being equal if two seedlings were both competing for a light source, the tallest one would win). Brown *et al* proposed that differences in seedling persistence in the shade of the forest canopy are highly influenced by species-specific abiotic and biotic interactions. Their experiments suggest that as seedlings, species trade-off the ability to grow rapidly in the high light environment found in tree-fall gaps (or free space) against the ability to persist and grow in shade. Thus, we define competition between species as the competition for the limiting resource of light. Hence 'more competitive' means 'better at competing for light'. Observations suggest that the majority of species will all fruit at the same time. These fruiting 'events' occur after a random interval of time, in general between 3-11 years. Less competitive species survive for progressively longer periods of time after a gregarious fruiting event. This leads to significant differences in the composition of the seedling bank over time after a fruiting event. Brown *et al* proposed that this special case of dispersal limitation (differences in species' seedling abundance over time) is more likely to account for co-existence of Dipterocarpaceae species than differences in growth responses to gaps

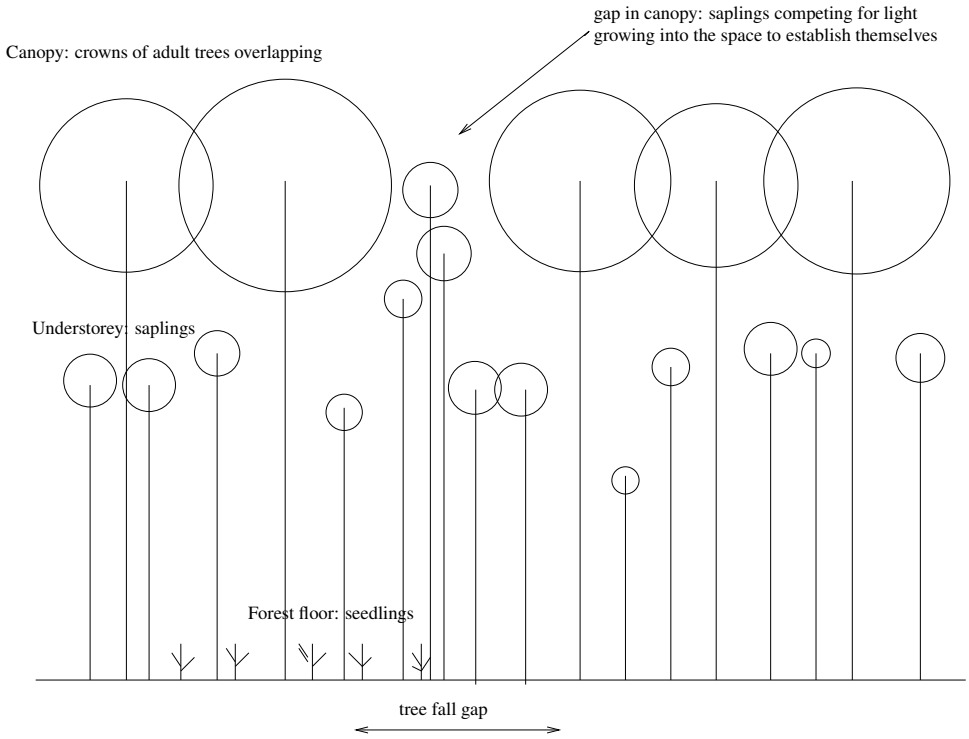


Figure 1.3: Idealised cross section of the rainforest

of different size, with stochastic and environmental factors interacting to determine species distribution and abundance.

Most hypotheses of rainforest diversity have assumed that the diversity is due primarily of competition between species, [1], [4] and [14]. In Chapter 2, we review a number of such models. In Chapters 3 - 5, we find that such models predict that one species will dominate. In Chapter 6, we use Brown's Hypothesis [5], namely that

> *We propose that an important mechanism for maintaining high diversity in the Borneo rainforest is the random mass fruiting events and the differing abilities of species to persist, as seedlings, after these events. It is not enough for the colonisation rate of each competitor to remain constant, we require decaying colonisation rates to describe the decay of numbers of seedlings in the seedling bank during the periods of time after a fruiting events.*

We develop and analyse mathematical models of competition to determine whether or not they can explain the diversity observed in real rainforests, both without and with seedling population decay.

Chapter 2

Literature review of the methods which may be applicable to modelling diversity and competition in tropical rainforests

2.1 Introduction

Tropical forests require special modelling techniques, as they may have many species, indeterminate ages, and a wide range of growth habits. An ideal model systems of equations would ensure reliable predictions over all tree sizes, sites and stand conditions. One significant constraint in ecological modelling is the inability to manipulate ecosystems and detect responses over spatial and temporal scales that have any practical relevance. This is especially true in the study of tropical rainforests. Several existing models could be fused for tropical rainforests if suitable data were available. We shall review several areas of interest with possible application to tropical forests. Specifically, we consider, in turn, a deterministic approach, a probabilistic approach and spatially explicit models. These models have been applied primarily to populations of plants, however similar techniques are also employed in viral dynamics and also insect population dynamics, which we shall also discuss briefly.

2.2 Deterministic models

A very influential paper on the use of deterministic models of competition and biodiversity is due to Tilman (1994) [28], which has been cited over 150 times since its publication, and it will be the starting point for our modelling in the later chapters of this dissertation.

2.2.1 Tilman: spatial theory

The model presented is drawn from metapopulation dynamics, and is frequently used for modelling ecosystems. Considering a single sessile species living in a habitat composed of distinct sites, where a site can be occupied by at most one adult, then the death of an adult would open up a gap for colonists. The dynamics of site occupancy would depend on the mortality rate and the colonisation rate of the species. The dynamics of the entire habitat are the sum of the individual processes of death (mortality) and replacement (colonisation) in each site.

2.2.1.1 Single species dynamics

If p is the proportion of sites occupied by a species, i.e. its abundance, then a simple model for the dynamics of site occupancy is:

$$\frac{dp}{dt} = cp(1-p) - mp, \tag{2.1}$$

where c is the colonisation (or proliferation) rate and m the mortality (local extinction) rate. Propagules are assumed to disperse randomly among all sites. The rate of seedling production by the occupied sites, cp, is multiplied by the fraction of unoccupied sites, $(1-p)$, to give the rate of production of newly colonised sites. The mortality rate, m, is multiplied by the proportion of occupied sites, giving a density-independent rate at which sites become vacant. A site becomes vacant when the occupant dies.

This model is directly analogous to logistic growth and has a globally stable equilibrium point. Equilibria or steady states occur when $\frac{dp}{dt} = 0$, i.e. there is no change in the species abundance. For the model (2.1) there are two steady state values for the proportion of the habitat occupied at equilibrium, namely, 0, and

$$p^* = 1 - \frac{m}{c}. \tag{2.2}$$

This shows that a species can persist in a habitat only if its colonisation rate, c, is greater than its mortality rate, m. Another interesting feature is that in this model, a sessile species can never fill the habitat ($p = 1$), for this would require either m to be zero (immortal) or c to be infinite, neither of which is biologically possible. The rest of Tilman's modelling assumes that for a number of interacting species $m_i > 0$ and c_i is finite, where m_i and c_i are the mortality rate and proliferation rate, respectively, of species i. These values mean that a species must leave a portion of the sites open for colonisation by another species.

2.2.1.2 Competition between two species

Assuming that we have a superior (species 1) and an inferior competitor (species 2) in a habitat, and that the superior competitor always displaces the inferior when they both occur in a site, and that the inferior competitor can neither invade into nor displace the superior competitor from a site, then the following equations can be used to model the dynamics:

$$\frac{dp_1}{dt} = c_1 p_1(1-p_1) - m_1 p_1 \tag{2.3}$$

$$\frac{dp_2}{dt} = c_2 p_2(1-p_1-p_2) - m_2 p_2 - c_1 p_1 p_2. \tag{2.4}$$

Note that the equation for the superior competitor (2.3) is as if it lived as a species on its own. The inferior competitor can only colonise sites where both it and species 1 are absent (the $(1-p_1-p_2)$ term in (2.4)), however species 1 can displace species 2 (the $-c_1 p_1 p_2$ term in (2.4)). Linear stability analysis of the equilibrium points shows that if both species have the same mortality rate then the system is globally stable. This is because the best competitor grows logistically until it approaches its equilibrial abundance, then species 2 grows logistically to equilibrium. The superior competitor must have a colonisation rate of $c_1 = \frac{m_1}{1-p_1^*}$ to attain an equilibrial abundance of $p_1^* \ \ (0 < p_1^* < 1)$. The inferior competitor can only invade if $\frac{dp_2}{dt} > 0$ for $p_1 = p_1^*$, that is, if

$$c_2 > c_1 \left(\frac{p_1^*}{1-p_1^*} + \frac{m_2}{m_1} \right). \tag{2.5}$$

In this case, the equilibrium point at which both species have strictly positive abundance is locally stable.

2.2.1.3 Multiple species competition

The model for two species ((2.3) and (2.4)) can be extended to n equations for n species. Ordering the species by competitive ability, such that p_1 is the most competitive and p_n the least competitive species, the dynamics for the ith species is:

$$\frac{dp_i}{dt} = c_i p_i \left(1 - \sum_{j=1}^{i} p_j \right) - m_i p_i - \sum_{j=1}^{i-1} c_j p_j p_i, \quad i = 1, \ldots, n. \tag{2.6}$$

The dynamics of each species, $(i = 1, \ldots, n)$, depends on the colonisation, the mortality and the displacement of other (less competitive) species. At equilibrium (with (2.6) set to zero for each i) the ith species occupies the following proportion of the habitat:

$$p_i^* = 0 \ \text{ or } \ p_i^* = 1 - \frac{m_i}{c_i} - \sum_{j=1}^{i-1} \left[p_j^* \left(1 + \frac{c_j}{c_i} \right) \right]. \tag{2.7}$$

The abundance of the ith competitor is reduced by the summed abundances of all its superior competitors and by the summed ratio of the rate at which it is displaced by superior competitors to its dispersal rate.

Tilman gives some numerical simulations showing species dynamics for 2, 4 and 40 species. By varying the colonisation rates and the mortality rates, he shows that different species can have the greatest abundance at a steady state, even if the species is not the best competitor.

2.2.2 Habitat destruction

Tilman *et al* [30] have also extended Tilman's [28] original model to include habitat destruction. Habitat destruction is the major cause of species extinction. Dominant species are often considered to be free from this threat, but the model described indicates that species initially abundant in undisturbed habitat fragments can be the most susceptible to eventual extinction. Even moderate habitat destruction causes a time delayed but deterministic extinction of species in remnant patches. Since such extinctions occur generations after fragmentation, they represent a future ecological cost of current habitat destruction: i.e. a debt.

If D is taken to be the proportion of sites permanently destroyed and included in the model (2.6), then the following equation describes the dynamics of the ith species:

$$\frac{dp_i}{dt} = c_i p_i \left(1 - D - \sum_{j=1}^{i} p_j\right) - m_i p_i - \sum_{j=1}^{i-1} c_j p_j p_i. \tag{2.8}$$

The equilibrial abundance (when $\frac{dp_i}{dt} = 0$) is:

$$p_i^* = 0 \;\text{ or }\; p_i^* = 1 - D - \frac{m_i}{c_i} - \sum_{j=1}^{i-1} \left[p_j^* \left(1 + \frac{c_j}{c_i}\right)\right]. \tag{2.9}$$

The best competitor has $p_1^* = 1 - D - \frac{m_1}{c_1}$ (the $p_i^* = 0$ is unstable if a strictly positive equilibrium point exists). It undergoes deterministic extinction once a proportion of the habitat equal to its proportional abundance in a virgin habitat is destroyed. If $D = 0$ this model reduces to that of Tilman's [28].

2.2.3 Imperfect trade-offs

The models in Tilman [28] and Tilman *et al* [30] assume that there is a tight trade off between competitive and colonisation abilities. This trade-off implies that species ranked high in competitive ability will be ranked low with respect to dispersal. Such a strict trade-off is

unlikely to occur in nature although it has a usefulness in examining general trends. There are many examples of deviations from perfect trade-offs in nature. Banks [2] examines how robust the 'extinction debt phenomenon' is to imperfect trade-offs.

In Banks' paper, the assumption of the perfect trade-off is weakened, and predation is neglected. The dispersal pattern is described as a global phenomenon, without any spatial detail. The system of differential equations (2.8) is solved numerically (in MATLAB). All the species are assumed to have identical mortality rates and initial abundances. The simulation starts with a perfect trade-off and then values are randomly added or subtracted from the colonisation rate of each competitively ranked species. With the inclusion of the scatter, it is found that although the extinction debt phenomenon is not eliminated by the presence of imperfect trade-offs, the loss of species occurs earlier (with less habitat destruction) and more linearly than with a perfect trade-off. Clearly if too much habitat is lost then the extinction of species is inevitable.

2.3 Probabilistic approach

2.3.1 Recruitment limitation

Hurtt & Pacala [18] introduce a model, again based on Tilman's [28], viewing the interaction between species as a local competition between juveniles of different species for environmentally variable sites left vacant by the random death of adults.

The space within the habitat is partitioned into sites, as in Tilman's model, and each contains at most one adult. The local environmental conditions vary independently in time and space and the relative competitive abilities of the juveniles depend on the local conditions. A juvenile which captures a vacant site is the strongest competitor present under the environmental conditions in the site at a particular time. It is assumed that juveniles are dispersed randomly over the habitat and immediately die unless they capture a vacant site. The model derived is as follows:

$$\Delta X_i = -d_i X_i + \left[\sum_{j=1}^{n} d_j X_j + 1 - \sum_{j=1}^{n} X_j \right] R_i(X_i) W(\bar{X}_i), \quad i = 1, \ldots, n, \tag{2.10}$$

where n is the number of different species, X_i is the proportion of sites occupied by species i at time t, d_i is the adult death rate of species i, $R_i(X_i)$ is the probability that a juvenile is present in a site and $W(\bar{X}_i)$ is the probability that species i wins a vacant site given that it is present, where $\bar{X}_i = (X_1, \ldots, X_{i-1}, X_{i+1}, \ldots, X_n)$.

The adult death rate (d) is taken to be constant and identical for all species. The vacant space is the set of sites without an adult present. There are two sources of vacant space:

sites vacated due to the death of an adult ($d\Sigma X_j$), and the sites previously vacant (the fraction $1 - \Sigma X_j$).

It is assumed that per plant fecundity is constant and equal for all species (F). Assuming also that seed dispersal is random, the arrival of juveniles at a site is a Poisson random variable, then $R_i(X_i)$ is equal to one minus the probability that no juveniles are at a site, that is:

$$R_i(X_i) = 1 - e^{-FX_i}. \tag{2.11}$$

It is assumed that a species' competitive ability depends on the local environmental conditions. These conditions vary independently of time and space along a single environmental axis (E), with a constant probability density, $P(E)$. On the axis, a species 'niche position' is defined as the environmental conditions under which it is dominant over all potential competitors. The assumption is that a species will win a site if the environment is closer to the species niche position than that of any other species present, which is consistent with a range of mechanistic models of competition. Hence a species is absolutely dominant under the environmental conditions within its niche. A species will 'win-by-forfeit' if it captures a site with environmental conditions outside its niche in the absence of a more dominant but recruitment limited competitor.

The analysis in the paper, as a result of numerical simulations, suggests that recruitment limitation allows 'winning-by-forfeit' which lessens the effect of competitive asymmetries and slows population and community dynamics.

2.3.2 Effects of competitive asymmetry

Zhang & Lin [35] introduce a simplified version of Hurtt & Pacala's [18] model. It is clear, intuitively, that the time required for competitive exclusion increases as the competitive abilities of species become closer to each other. Hubbell [17] modelled the tropical rainforests under the extreme assumption of competitive equivalency. This is extended and the case of unequal competitive abilities are considered.

Again, space is partitioned into a fixed number of sites, each containing at most one adult, and sites are vacated by the random death of adults. Vacant sites are occupied because of competition between juveniles of different species. Sites are coupled by the dispersal of juveniles produced by adults. The model considers the stochastic dynamics of the focal species population in this finite habitat with K total individuals of all species, which are assumed to have different competitive abilities. Two species are considered, identical, except for per capita fecundity.

A slight variation on the original assumption could lead to a great decline in the persistence time of species. Since species cannot be ecologically identical in any real ecosystems, it is concluded that the validity of the community drift hypothesis is rather restricted.

2.3.3 High species richness

Yu *et al* [33] extend further the work of Zhang & Lin [35] by allowing tree mortality rates to differ across species, as is seen in natural communities. As a result, species persistence time decreases dramatically (much faster than predicted by Zhang & Lin) and the forest composition becomes highly deterministic. Long-lived species disappear much more slowly than short-lived ones. If tree deaths are used (rather than years) as a measure of time, this increases the estimate of persistence times. However, the calculated persistence times of tropical species (even for those in large forests) does not reach the time scale plausible for speciation.

2.3.4 Competition-colonisation model including niche hypothesis mechanism

Pacala & Rees [23] consider both a stochastic model and a deterministic model to describe population dynamics. The former uses the competition-colonisation hypothesis that early successional species are able to persist because they colonise disturbed habitats before the arrival of late successional dominant competitors (winning-by-forfeit). The latter employs the niche hypothesis and modifies the competition-colonisation models to include this hypothesis. Analysis of the second model leads to suggestions for experiments to determine whether diversity is maintained primarily by the competition-colonisation mechanism, the niche mechanism, neither or both. Implications for management of biodiversity within communities are also discussed.

2.3.5 Sexual reproduction

Current competition theory predicts that species must be ecologically distinct in order to coexist stably in the same community. This prediction is based on the implicit assumption that the consequences of sexual reproduction can be ignored. The general assumption is that its inclusion only leads to problems (hastening competitive exclusion). Zhang & Hanski [34] suggest that sexual reproduction may also bring rare species an advantage in terms of the rate of per capita population growth.

The key result is that species-specific density dependence in population growth can occur when sexual reproduction is explicitly considered. Zhang & Hanski show that a density

dependent sex ratio and sexually transmitted diseases can all promote species coexistence without separate niches. The model proposed for two species (male and female) is as follows:

$$\frac{1}{N_i}\frac{dN_i}{dt} = \frac{b_i}{1+s_i(N_i)} - d_i(N_i) - \sum_{j=1}^{n} c_{ij}N_j(1+s_j) \tag{2.12}$$

Where b_i is the fertility, s_i the sex ratio of males to females and N_i the female population density. The first term on the right hand side of (2.12) represents the birth rate of daughters, the second the death rate of adult females and the final term represents the competition induced by the mortality, where c_{ij} are competition constants.

2.4 Other Models

2.4.1 Spatially explicit models

Tilman's [28] model can also be extended to include spatial variation. A system of non-linear partial differential equations is developed. Examples of this type of model include those due to Goldwasser *et al* [13] and Ruxton & Doebeli [25].

Goldwasser *et al* derive a model that achieves analytical tractability by neglecting the variability among individuals in the patterns of movement between locations, in favour of considering the ability to colonise or persist. The spatial variation includes diffusion and dispersal. The proportional abundance is now taken to be a function of two variables, both time and space, and (2.6) is adapted accordingly to become a partial differential equation (PDE). The two species model takes the form:

$$\frac{\partial p_1}{\partial t} = c_1 p_1(1-p_1) - m_1 p_1 \tag{2.13}$$

$$\frac{\partial p_2}{\partial t} = c_2 p_2(1-p_1-p_2) - m_2 p_2 - c_1 p_1 p_2 \tag{2.14}$$

(2.13) and (2.14) are solved together with a diffusion equation which incorporates the spatial variation.

Ruxton & Doebeli consider a spatial discretisation in one-dimension (separating local populations) and also discrete intervals of time during which a reproductive episode occurs, followed by migration and then the new conditions are taken as the starting values for the next time step (generation). The model produces transient behaviour lasting thousands of generations. It also predicts organised spatial heterogeneity across the system. In addition the model predicts that peripheral populations are subject to greater temporal variation than the interior.

MOSEL (MOdule for Spatially Explicit Landscapes), a version of the JABOWA-FORET model of the dynamics of establishment, growth, and death of forest trees that includes dispersal among cells, is used by Malanson [19] to gain some insight into the effects of colonisation and mortality. Comparisons of diversity are made for simulations of equal or variable dispersal probabilities among species and the occurrence or absence of density independent mortality on sites. It may be possible to use this module as an alternative to solving the system of non-linear PDEs resulting from the models developed above.

2.4.2 Age structured models

Clark & Ji [7] have developed a model to assess the consequences of fecundity and dispersal for population structure and diversity. In order to isolate the effects of fecundity and dispersal, gap models of three complexities are developed. The population density they consider can be described statistically, e.g. by means and variances, on a regional scale. The dynamics are summarised by:

$$\frac{\partial n}{\partial t} + \frac{\partial n}{\partial a} = -\left[\sum_{i=0}^{q} m_i(\cdot)\right] n(a,t) \tag{2.15}$$

where the density of cohorts $n(a,t)$ of age a at time t are exposed to q mortality agents characterised by rates m_i, at least one of which can be density dependent. Recruitment implies the following boundary condition:

$$n(0,t) = \int_{a_1}^{a_2} u(a,t)n(a,t)b(a,t)\mathrm{d}a, \tag{2.16}$$

for initial age distribution $n(0,t)$, where $u(a,t)$ is the distribution of patch ages, $b(a,t)$ the fecundity schedule, a_1, maturation age, and a_2, longevity.

Equation (2.16) is termed the 'seed' or 'initial density' which can assume a distribution of values dependent on the population structure and dispersal. The landscape density is:

$$E[N(t)] = \int_{0}^{a_2} u(a,t)n(a,t)\mathrm{d}a. \tag{2.17}$$

The analysis only considers equilibrium behaviour of the dynamics, i.e. at steady states.

The results of the analysis indicate that maturation age affects the mean and variance in seed rain. Populations with well-dispersed seed have a structure that is most sensitive to maturation age when disturbance is frequent. Longevity, however, has the greatest effect when it is short and disturbance rare. Fecundity and population structure affect both the mean and the variance in seed rain, but dispersal affects only the variance. Dispersal has important consequences on the time scales observed in many real forests. Most models of

forest tree dynamics assume a globally dispersed seed pool that is disconnected from the populations that produce the seed. This assumption leads to two opposing consequences for seed diversity. It will be artificially high due to continuous seed supply, and artificially low due to lack of sites where good competitors with restricted dispersal should be absent.

2.4.3 Dynamical systems approach to ecosystems

Problems concerned with described ecological variability are discussed by Stone & Ezrati [27]. They propose that non-linear systems theory and chaos may be of relevance for understanding pattern and change in ecosystems. The basic concepts involved are briefly outlined, including period doubling as a route to chaos, associated bifurcations, universality, sensitivity to initial conditions and attractors. The presence of a density dependent growth rate is generally a necessary (not sufficient) condition for chaos. A general discussion about methods employed and example populations from nature and where they might be used are discussed.

It is often assumed that plant populations will fluctuate in time and eventually reach a stable equilibrium, from which small perturbations will again lead back to the equilibrium state. However, this is not always the case when spatial variation is incorporated into models. For example the extinction debt phenomenon is non-linear and much more complicated than a linear model which may lead to chaos.

Morton & Law [21] model the sequential assembly of species into communities, using a notion of permanence for dynamical systems theory. Again this is a general discussion and gives a basic introduction to the sorts of systems of equations or maps that may result from modelling ecosystems. They find that communities built from species rich pools develop more slowly to invasion resistant states. Where species pools are rich in consumers, fewer basal species are found, even though specialisation by the consumers enables more basal species to exist locally. The invasion resistant states may be single communities or cyclic sequences of communities uninvadable by species not in the cycle. If species pools are made rich enough, they may cause saturation of local communities such that the number of species present becomes decoupled from the richness of the pool.

2.4.4 Virus dynamics

Decay characteristics of HIV-1 infected compartments with respect to drug therapy may yield similar dynamics to those of metapopulations in the rainforest, especially the models that incorporate mutations of the virus. Examples of research of this type are to be found in Perelson *et al* [24], Bonhoeffer *et al* [3] and Stilianakis *et al* [26].

Tilman's [28] model is also used to describe superinfection or metapopulation dynamics of virus strains. The notion of the metapopulation is similar to that described in rainforest dynamics, where many different strains contend for persistence. Again a strict hierarchy of competitive dominance is laid out. Superinfection represents an intermediate level of complexity: the more virulent strain of infection can take over a host that is already infected with a less virulent strain, but the host will, in effect, harbour only one strain of virus at any one time. Hence superinfection goes beyond single infection, allowing intra-host competition among strains. May & Nowak [20] consider the questions relating to the evolution of diversity. How many strains are present after a long time? The inclusion of vaccination in the model has direct comparison with the habitat destruction in the forest model described by Tilman *et al* [30].

Mosquer & Adler [22] have developed a model for the evolution of parasite virulence, focusing on computing the evolutionarily stable level of virulence favoured by trade-offs within a host and by competition for hosts, and deriving conditions under which strains with different virulence levels can coexist. The model is similar to that of May & Nowak [20] which is, in turn, based on Tilman [28]. Mosquer & Adler's results depend on the type of interaction between the disease strains, i.e. single infection, co-infection (when only two strains are present) or superinfection. They present a co-infection model with two strains and then derive the superinfection model as a limit where individuals are rapidly removed from the doubly infected class. The superinfection model allows take over of the host by the less virulent strain and new terms in the model take into account the possibility of increased mortality of doubly infected individuals.

The diseases are modelled as actors in an evolutionary theatre. Questions asked include: when can several diseases live together either in the same host or population of hosts; under what circumstances should diseases reduce the degree of harm caused to the host? Mosquera & Alder's results indicate the potential for ecosystems to support a diversity of organisms and act as a paradigm for 'prudent' resource exploitation.

The results of the co-infection model depend on the shape of the co-infection function. When the co-infection function is discontinuous neither the co-infection model nor the superinfection limit can support an evolutionarily stable virulence level. Piecewise differentiable and differentiable co-infection functions produce qualitatively different results. It is proposed by Mosquera & Alder that these more general cases should be used to study the evolution of virulence when other mechanisms are included in the model.

What can be learned from virus dynamics that is applicable to rainforest dynamics? It appears as though the basic models are similar and that few different results have been found. There is the possibility that the idea superinfection might be applied to rainforests

when one species takes over, however this is not observed in the field and thus its usefulness would be limited.

2.4.5 Population dynamics of insects

There has been a substantial amount of research into the behaviour of population dynamics of the flour beetle *Tribolium*. We shall start by looking at Costantino *et al* (1995) [8] who show that simple non-linear models can generate fixed points, periodic cycles (the population number oscillates between a finite number of values) and aperiodic oscillations in population abundance without any external environmental variation.

It is shown that shifts in demographic parameters (eg survival, fecundity) can move the population from one behaviour to another. A joint theoretical and experimental study was carried out to test the hypothesis that changes in the demographic parameters (in this case mortality rate) cause predictable changes in the nature of the population fluctuations.

A simple model is developed of a map:

$$L_{t+1} = bA_t \exp(-c_{ea}A_t - c_{el}L_t) \tag{2.18}$$

$$P_{t+1} = L_t(1-\mu_l) \tag{2.19}$$

$$A_{t+1} = P_t \exp(-c_{pa}A_t) + A_t(1-\mu_a) \tag{2.20}$$

where L_t is the number of feeding larvae, P_t, the number of non-feeding larvae, pupae, and callow adults and A_t the number of mature adults all at time unit t (assumed discrete). The unit of time was 2 weeks. The quantity b is the number of larval recruits per adult per unit of time in the absence of cannibalism. The fractions μ_l and μ_a are the larval and adult rates of mortality, respectively, in one time unit. The exponential non-linearities account for the cannibalism of eggs by both larvae and adults and the cannibalism of pupae by adults. The fractions $\exp(-c_{el}L_t)$ and $\exp(-c_{ea}A_t)$ are the probabilities that an egg is not eaten in the presence of L_t larvae and A_t adults in one unit time. The fraction $\exp(-c_{pa}A_t)$ is the survival probability of a pupa in the presence of A_t adults in one time unit. The model was derived by fitting time series data and then converted to a stochastic model. Similar work is carried out by Dennis *et al* [11] with more rigorous statistical analysis included.

Costantino *et al* (1997) [10] extend their work from 1995 [8] and find that chaotic behaviour is observed under certain laboratory protocols. The dynamics show transitions from equilibrium states to periodic cycles, to quasi-periodic cycles (fluctuations in population numbers on a stable attractor) to chaos (sensitive dependence to initial conditions) as the adult stage recruitment rate is manipulated. The experimental results correspond to

those predicted by the mathematical model. The model is a map of stochastic difference equations:

$$L_{t+1} = bA_t \exp(-c_{ea}A_t - c_{el}L_t + E_{1t}) \quad (2.21)$$

$$P_{t+1} = L_t(1-\mu_l)\exp(E_{2t}) \quad (2.22)$$

$$A_{t+1} = [P_t \exp(-c_{pa}A_t) + A_t(1-\mu_a)]\exp(E_{3t}), \quad (2.23)$$

where the terms E_{it} $(i = 1, 2, 3)$ are random noise variables assumed to have a joint multivariate normal distribution.

The effect of altering of the amount of habitat (by changing the volume of flour) are investigated in Henson & Cushing [16] and Costantino *et al* (1998) [9]. They found that the populations exhibited resonance and periodic orbits which agreed with the prediction of the mathematical models.

A similar time decay of parameters is also observed in the decay of seedling abundances of rainforest trees. We will incorporate this into the proliferation rates in Chapter 6.

2.5 Conclusion

In this chapter we have briefly summarised the variety of methods that might be applicable to modelling competition and diversity in tropical rainforests. We shall begin with Tilman's model [28], and then use the other models to inform our adaptation of his model and our determination of parameter values. We shall return to some of the issues raised in this chapter when future possible work is discussed in the concluding chapter.

Chapter 3

Two Species Model

3.1 Introduction

We shall start from Tilman's model [28]. We have to adapt his model because our trees (in the rainforest) do not displace one another (the $-c_1 p_1 p_2$ term in (2.4)). We also need to incorporate a 'gap' term and an equation to ensure that the total proportional abundance of all trees is less than one, and also that the total proportional abundance including the gap is equal to one. The more competitive species is defined to be the one whose seedlings, if present, can grow fastest into a gap. We begin by investigating a system of two competing tree species. Such a system lends itself to a complete mathematical study of linear and global stability and will help in gaining a deeper understanding of this type of interaction before including more species.

3.2 Model and Determination of Steady States

The two species system is:

$$\begin{aligned}
\frac{dp_1}{dt} &= c_1 p_1 g - m_1 p_1 && (3.1)\\
\frac{dp_2}{dt} &= c_2 p_2 g(1-p_1) - m_2 p_2 && (3.2)\\
\frac{dg}{dt} &= -c_1 p_1 g - c_2 p_2 g(1-p_1) + m_1 p_1 + m_2 p_2 && (3.3)\\
1 &= p_1 + p_2 + g, && (3.4)
\end{aligned}$$

where $p_1(t)$ and $p_2(t)$ are the proportional abundances of species 1 and 2, respectively, at time t, and $g(t)$ is the proportional abundance of available free space (gaps). c_i is the colonisation rate and m_i is the mortality (local extinction) rate of species i. Adding (3.1) - (3.3), we have that $p_1 + p_2 + g = constant$, which we take to be 1, leading to equation (3.4).

state	p_1^0	p_2^0
(a)	0	0
(b)	0	$1 - \frac{m_2}{c_2}$
(c)	$1 - \frac{m_1}{c_1}$	0
(d)	$1 - \frac{m_2 c_1}{c_2 m_1}$	$\frac{m_2 c_1}{c_2 m_1} - \frac{m_1}{c_1}$

Table 3.1: Steady states of model (3.1) - (3.4)

Initially we follow Tilman [28] in taking the c_i to be constant to see if this simple model will allow the diversity described in Chapter 1. Species 1 is defined to be the most competitive species, that is the one whose seedlings will grow the fastest to reach the light (in a tree fall gap). First considering equation (3.1), propagules are assumed to be dispersed randomly among all sites. The rate of propagule production by the occupied sites of species 1, $c_1 p_1$, is multiplied by the proportion of sites that are unoccupied, g, to give the rate of production of newly colonised sites (Law of Mass Action). The mortality rate, m_1 is multiplied by the proportion of sites occupied by species 1, p_1, to give the rate at which the sites become vacant. A site is vacated when the individual occupying it dies.

The introduction of a second species does not affect the dynamics of species 1, since the new species is an inferior competitor. We assume that the superior competitor always displaces the inferior competitor when both are competing for a site. The inferior competitor, species 2, can then only colonise when species 1 is absent and there is a vacant site, leading to the term $g(1 - p_1)$ in (3.2). The proportion of vacant sites, gaps, decreases due to species colonisation and increases due to species death.

Equation (3.3) decouples from the system and using (3.4) we are left with a system of two first order non-linear ordinary differential equations:

$$\frac{dp_1}{dt} = c_1 p_1(1 - p_1 - p_2) - m_1 p_1 \tag{3.5}$$

$$\frac{dp_2}{dt} = c_2 p_2(1 - p_1 - p_2)(1 - p_1) - m_2 p_2. \tag{3.6}$$

The steady states of the system are found by setting:

$$\dot{p_1} = 0 = \dot{p_2},$$

where $\dot{}$ denotes $\frac{d}{dt}$. The four possible steady states are given in Table (3.1).

The different steady states (or equilibrium points) correspond to different proportional abundances of the species. The state (a) corresponds to both species dying out and no trees being present. (b) corresponds to species 1 being totally dominated by the less competitive species 2, and there is no coexistence, only trees from species 2 present. Similarly in (c) the

more competitive species 1 dominates species 2 causing it to die out completely. Finally in (d) both species coexist and both have a non-zero abundance at the steady state. In a rainforest many species coexist and it is a steady state of type (d) that we are trying to reproduce. The feasibility and stability of these steady states will be investigated below.

3.3 Linear Stability Analysis

We now carry out linear analysis of the steady states in Table (3.1) in the standard way. Consider the system for general functions f and h:

$$\dot{p_1} = f(p_1, p_2) \tag{3.7}$$

$$\dot{p_2} = h(p_1, p_2). \tag{3.8}$$

Linearising about the general steady state (p_1^0, p_2^0) we have, using a Taylor expansion,

$$\dot{\widetilde{p_1}} = a\widetilde{p_1} + b\widetilde{p_2}, \quad \dot{\widetilde{p_2}} = c\widetilde{p_1} + d\widetilde{p_2},$$

where $p_i = p_1^0 + \widetilde{p_i}$, $i = 1, 2$, $a = \frac{\partial f}{\partial p_1}$, $b = \frac{\partial f}{\partial p_2}$, $c = \frac{\partial h}{\partial p_1}$ and $d = \frac{\partial h}{\partial p_2}$, where we assume $|\widetilde{p_i}| \ll 1$ so that we can ignore higher order terms. We may write this as:

$$\begin{pmatrix} \dot{\widetilde{p_1}} \\ \dot{\widetilde{p_2}} \end{pmatrix} = \mathbf{J} \begin{pmatrix} \widetilde{p_1} \\ \widetilde{p_2} \end{pmatrix}$$

where

$$(J)_{ij} = \frac{\partial \dot{p_i}}{\partial p_j}(p_1^0, p_2^0).$$

For notational simplicity we drop the tildes.

The general solution of this linear system is of the form:

$$\begin{pmatrix} p_1 \\ p_2 \end{pmatrix} \propto \begin{pmatrix} r \\ s \end{pmatrix} e^{\lambda t} \tag{3.9}$$

where $\begin{pmatrix} r \\ s \end{pmatrix}$ is parallel to the eigenvector corresponding to the eigenvalue, λ, of the Jacobian matrix, $\mathbf{J}$. Here:

$$\mathbf{J} = \begin{pmatrix} (1 - 2p_1 - p_2) - \frac{m_1}{c_1} & -p_1 \\ -p_2(2 - 2p_1 - p_2) & (1 - p_1)(1 - p_1 - 2p_2) - \frac{m_2}{c_2} \end{pmatrix} \tag{3.10}$$

evaluated at the steady state (p_1^0, p_2^0). The eigenvalues are calculated from $|\ \mathbf{J} - \lambda \mathbf{I}\ | = 0 = d(\lambda)$. For ease of notation we define $\gamma_i = \frac{m_i}{c_i}$ for $i = 1, 2$. The eigenvalues for each steady state are calculated and shown in Table (3.2), where $\hat{\lambda_1}$ and $\hat{\lambda_2}$ (calculated in Maple [6]) are given by:

state	p_1^0	p_2^0	λ_1	λ_2
(a)	0	0	$1-\gamma_1$	$1-\gamma_2$
(b)	0	$1-\gamma_2$	0	$\gamma_2-\gamma_1$
(c)	$1-\gamma_1$	0	γ_1-1	$\gamma_1^2-\gamma_2$
(d)	$1-\frac{\gamma_2}{\gamma_1}$	$\frac{\gamma_2}{\gamma_1}-\gamma_1$	$\hat{\lambda_1}$	$\hat{\lambda_2}$

Table 3.2: Steady states of (3.5) - (3.6) and eigenvalues of the linearised system, see text for details

$$\begin{aligned}\hat{\lambda_1} &= \frac{1}{2\gamma_1^2}(-\gamma_1^2-\gamma_1^4+\gamma_1\gamma_2+\gamma_2^2+\sqrt{}(\gamma_1^4-2\gamma_1^6-2\gamma_1\gamma_2-\gamma_1^2\gamma_2^2+\gamma_1^8 \\ &\quad -2\gamma_1^5\gamma_2-2\gamma_1^4\gamma_2^2+2\gamma_1\gamma_2^3+\gamma_2^4-4\gamma_1^3\gamma_2^2+4\gamma_1^4\gamma_2)) \qquad (3.11)\\ \hat{\lambda_2} &= \frac{1}{2\gamma_1^2}(-\gamma_1^2-\gamma_1^4+\gamma_1\gamma_2+\gamma_2^2-\sqrt{}(\gamma_1^4-2\gamma_1^6-2\gamma_1\gamma_2-\gamma_1^2\gamma_2^2+\gamma_1^8 \\ &\quad -2\gamma_1^5\gamma_2-2\gamma_1^4\gamma_2^2+2\gamma_1\gamma_2^3+\gamma_2^4-4\gamma_1^3\gamma_2^2+4\gamma_1^4\gamma_2)) \qquad (3.12)\end{aligned}$$

3.4 Feasibility & Stability of Steady States

The p_i represent proportional abundances of rainforest tree species. Therefore to be a feasible state, both p_1 and p_2 must be non-negative. For example if we look at case (a) this is feasible for all values of γ_1 and γ_2. For steady state (b) we require $1-\gamma_2>0$ for feasibility, that is $\gamma_2<1$, and similarly for steady state (c) we require $\gamma_1<1$. For steady state (d) we need $1-\frac{\gamma_2}{\gamma_1}>0$ and $\frac{\gamma_2}{\gamma_1}-\gamma_1>0$ combining the two inequalities together this gives $0<\gamma_1^2<\gamma_2<\gamma_1<1$.

Steady states may be classified by their stability eigenvalues (calculated from $d(\lambda)$ above). If there exists at least one eigenvalue with real part greater than zero, then from equation (3.9), there are solutions that are growing exponentially and hence the steady state is linearly unstable. In order for a steady state to be linearly stable, both eigenvalues must have a negative real part. For the equilibrium points given by (a), (b) and (c) in Tables (3.1) and (3.2), calculations to find the parameter range for stability are simple, that is where $\gamma_1,\gamma_2>1$ for steady state (a), $\gamma_2>\gamma_1$ for steady state (b) and $\gamma_1>1$ with $\gamma_1^2>\gamma_2$ for steady state (c). However in case (d), it is not obvious by inspection how to determine the sign of the (real part of the) eigenvalues for the parameter values in the feasibility region. Therefore plots of $\hat{\lambda_1}$ and $\hat{\lambda_2}$ are used. The results are shown in Figure (3.1). Figure (3.1) shows the sign of each of the eigenvalues as the parameters, γ_1 and γ_2 vary, cyan for real part positive and white for real part negative. The boundaries of the feasibility region for

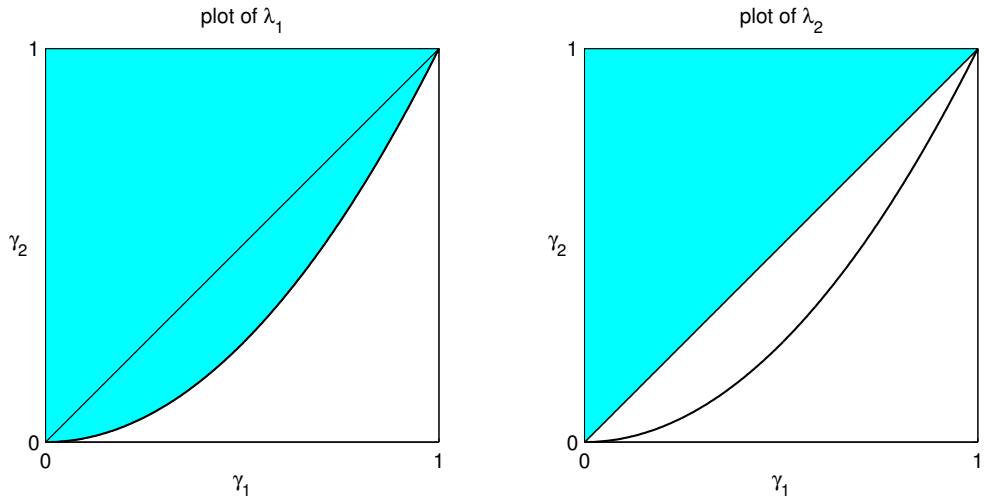


Figure 3.1: Plot of $\hat{\lambda_1}$ and $\hat{\lambda_2}$ showing the sign of the real part of the eigenvalues, cyan for $\mathbb{R}(\hat{\lambda_i}) \geq 0$, and white for $\mathbb{R}(\hat{\lambda_i}) < 0$ within the feasibility region (black lines show the boundaries).

steady state (d) are shown by black solid lines. From Figure (3.1) we can see, that although $\mathbb{R}(\hat{\lambda_2}) < 0$ in the region $\gamma_1^2 < \gamma_2 < \gamma_1$, the eigenvalue $\mathbb{R}(\hat{\lambda_1}) > 0$ in this region. Hence the steady state (d) is unstable for all feasible parameter values.

The results for feasibility and stability are collected and summarised in Figure (3.2). For example, in the region (2) we can see that $0 < \gamma_1 < \gamma_2 < 1$ and therefore (a) is a feasible steady state but linearly unstable. This is also the case for (b) since $\gamma_2 > \gamma_1$ and $\gamma_2 < 1$. Steady state (c) is stable ($\gamma_1 < 1$ and $\gamma_2 > \gamma_1^2$), (d) is unfeasible because $\frac{\gamma_2}{\gamma_1} > 1$.

3.5 Phase Plane Analysis

The above analysis determines the local behaviour near equilibria. To investigate the global behaviour, we now consider the phase plane of the system. The nullclines are found from setting equations (3.5) and (3.6) to zero. The intersections of the nullclines from the different equations give us the location of the steady states. The nullclines are given by: $p_1 = 0$, $p_2 = 0$, $p_2 = 1 - p_1 - \gamma_1$ and $p_2 = 1 - p_1 - \frac{\gamma_2}{1-p_1}$. The nullclines and the feasible steady states are sketched in the (p_1, p_2)-plane in Figure (3.3) with a different sketch for each of the six regions of the parameter space, marked out in Figure (3.2), (indicated by the shaded area in the (γ_1, γ_2)-plane). The stability of the steady states are indicated by their colour, with red (unstable) and green (stable).

Actual example phase planes with trajectories over time, for the six different regions in parameter space, are shown in Figure (3.4). The curves depicted in Figure (3.4) are known

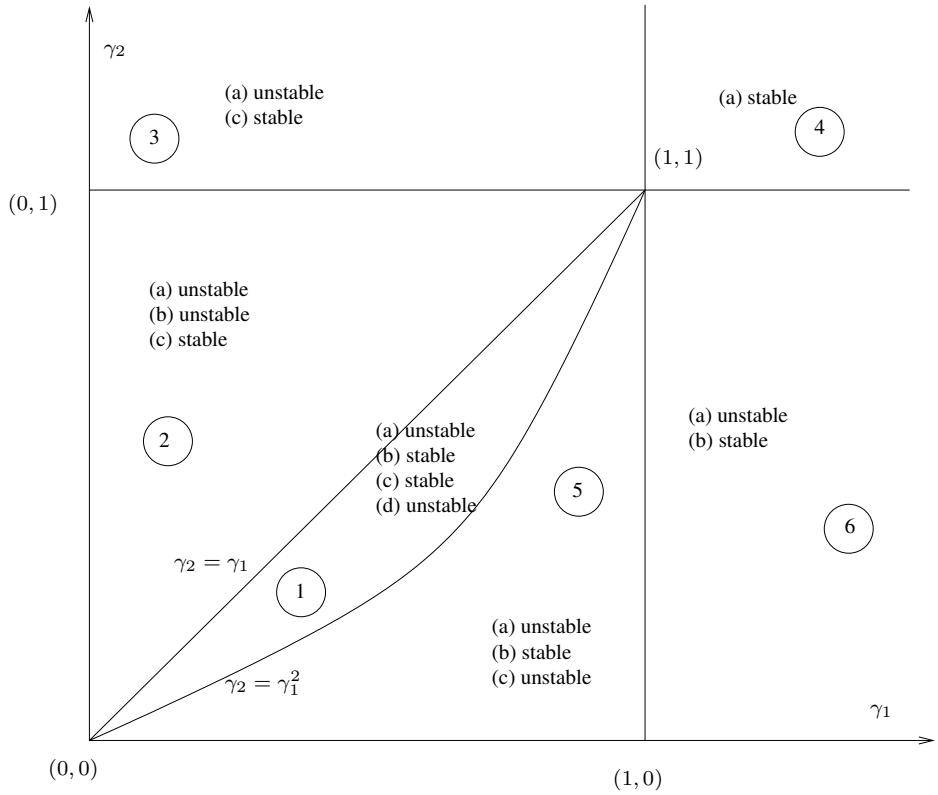


Figure 3.2: Stability & feasibility regions, see text for details

as the phase paths or trajectories corresponding to equations (3.5) and (3.6). Each trajectory corresponds to a particular possible motion of the system. These are found by running a numerical simulation, solving the differential equations (3.5) and (3.6) using MATLAB [15] `ode45` (an explicit, one-step Runge-Kutta medium order (4-5) ode solver). The parameter sets chosen in each case are taken from each of the six regions in the parameter space and can be found in Table (3.3). The initial conditions for the trajectories shown in Figure (3.4) are given in Table (3.4). The full lines represent trajectories, dotted lines represent nullclines. In the case of region (4) the dot-dashed line represents the line $p_1 + p_2 = 1$. The steady states are represented again by green (stable) and red (unstable) dots.

3.6 Conclusion

In the two species case, this model (Equations (3.5) and (3.6)) does not support a stable steady state with both species being non-zero, for any parameter set. In the rainforest many species coexist together and if this model cannot predict such dynamics, for two species alone, then its validity may be questioned. In order to determine whether the model is a viable one for describing rainforest tree dynamics we need to consider the three species model and its extension into larger numbers of species. Whether or not we can generalise

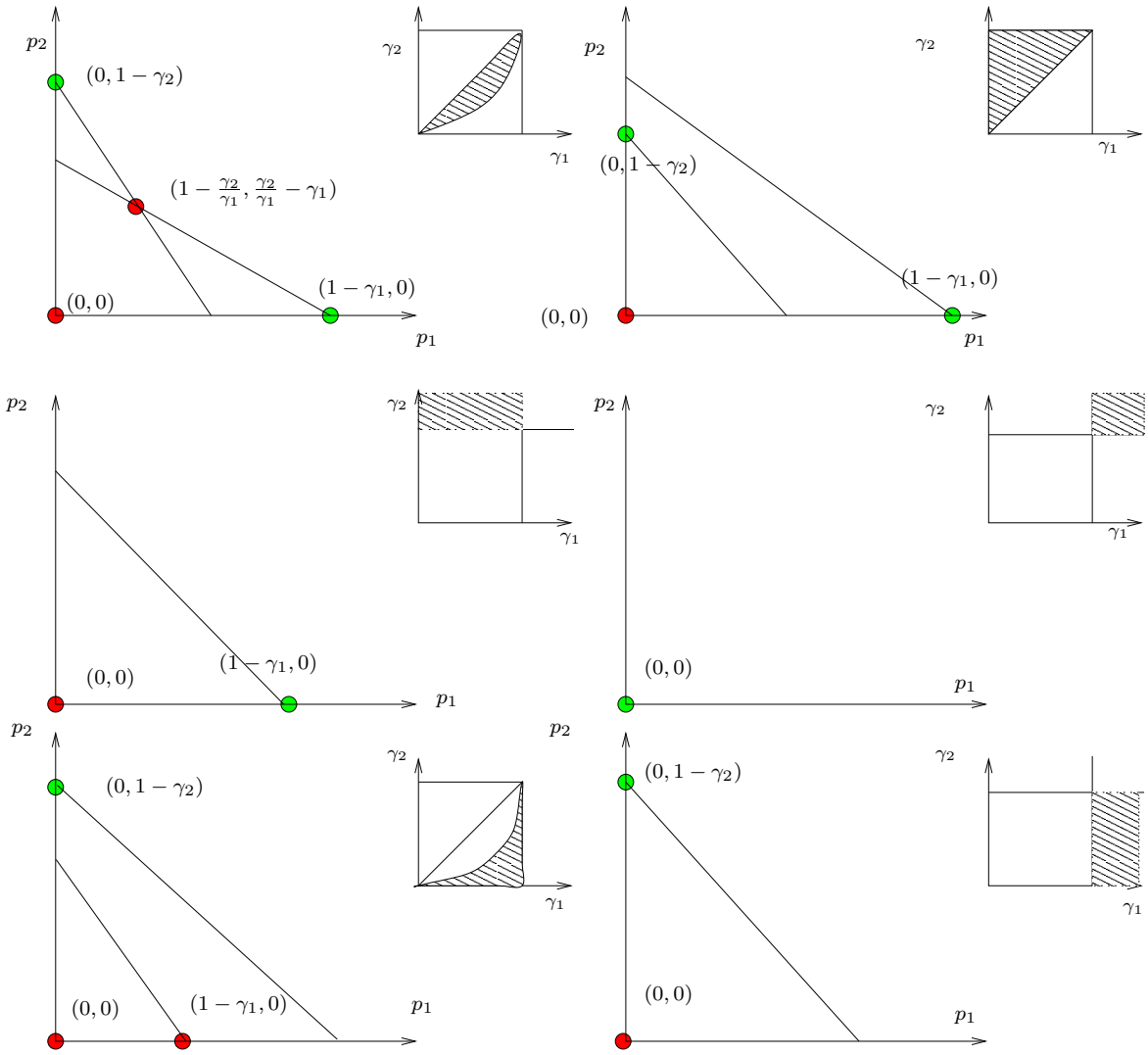


Figure 3.3: Nullclines & steady states for different regions within the parameter plane (γ_1, γ_2)

the model into n dimensions remains to be discussed in the following chapters. If indeed we can generalise that all models reduce to the two species case and hence predict no coexistence, we can abandon this model and look into other possibilities to describe the dynamics. Another mechanism to be included may be the mass fruiting events that occur in the rainforest at random intervals. This may be the mechanism that allows such diversity and richness of species.

In the next chapter we shall go on to investigate the extension of the model to three species.

region	γ_1	γ_2
1	0.40	0.30
2	0.50	0.75
3	0.50	1.20
4	1.20	1.20
5	0.50	0.20
6	1.20	0.50

Table 3.3: Parameter sets chosen for numerical simulations shown in Figure (3.4) for regions in Figure (3.2)

region	initial conditions						
1	p_1	0.050	0.050	0.050	0.010	0.050	0.025
	p_2	0.006	0.050	0.100	0.050	0.075	0.010
2	p_1	0.050	0.030	0.010	0.010	0.025	
	p_2	0.050	0.450	0.100	0.350	0.010	
3	p_1	0.050	0.030	0.010	0.010	0.025	
	p_2	0.050	0.450	0.100	0.350	0.010	
4	p_1	0.700	0.200	0.030	0.010	0.010	0.450
	p_2	0.100	0.700	0.800	0.100	0.350	0.450
5	p_1	0.050	0.450	0.050	0.010	0.300	0.025
	p_2	0.006	0.010	0.100	0.050	0.050	0.010
6	p_1	0.250	0.110	0.010	0.200	0.150	
	p_2	0.050	0.300	0.050	0.100	0.020	

Table 3.4: Initial conditions chosen for numerical simulations shown in Figure (3.4)

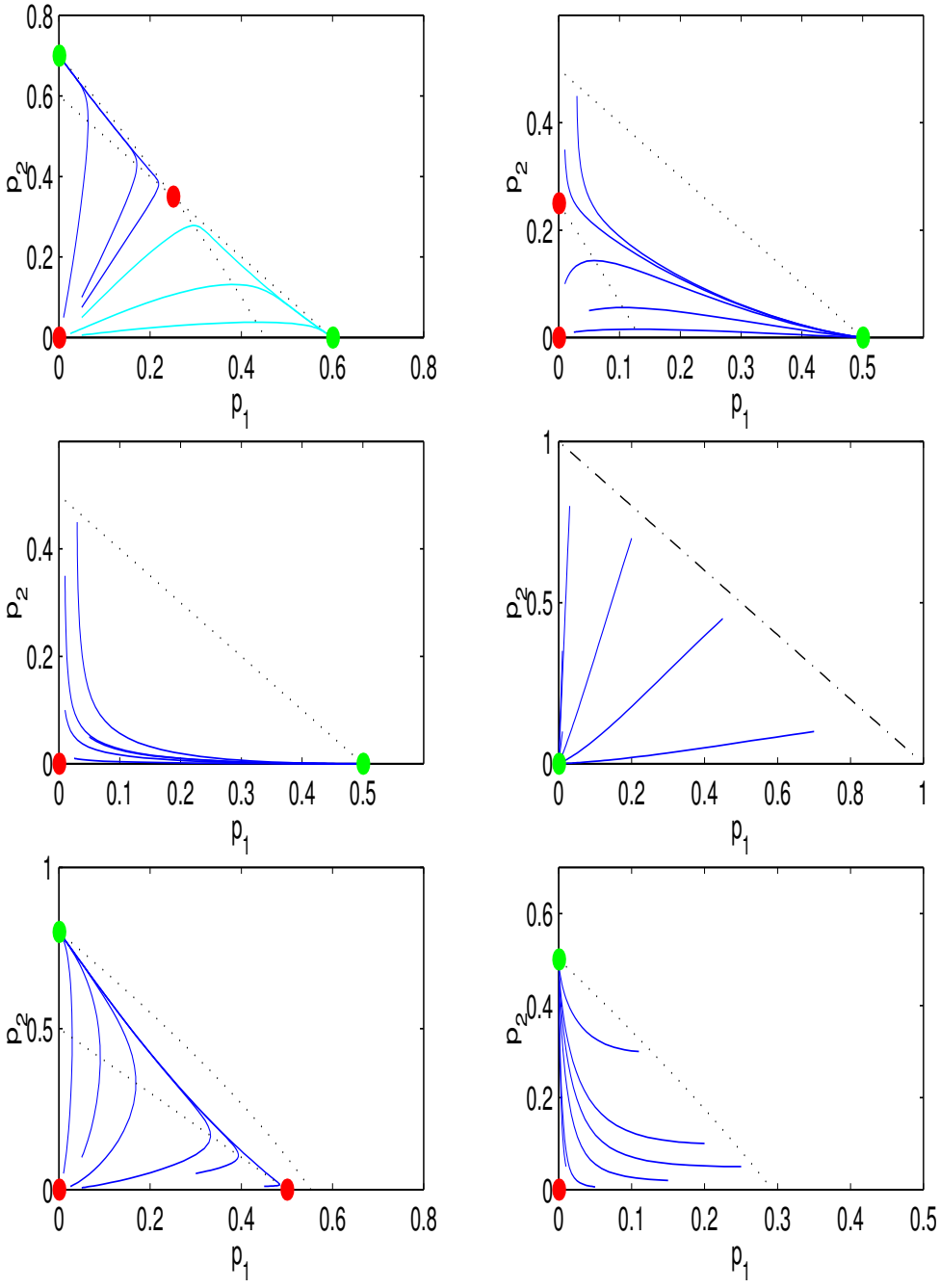


Figure 3.4: Phase planes in the different regions of the parameter space (γ_1, γ_2). The top left hand panel corresponds to region 1 and follow the same order as Figure (3.3).

Chapter 4

Three Species Model

4.1 Introduction

In the previous chapter we investigated in detail our model for two species and found that the model does not support coexistence of species. Now was shall determine whether the addition of another species can result in stabilising a steady state supporting all species with a positive abundance.

4.2 Model and Determination of Steady States

The three species model is a very simple extension of that seen in Chapter 3 (equations (3.1)-(3.3)). The inclusion of a less competitive species simply means the proportion of free space changes and the competitive interactions between species are slightly altered. If we assume that species 3 is less competitive than the first two then the system of equations is as follows:

$$\dot{p_1} = c_1 p_1 g - m_1 p_1 \tag{4.1}$$

$$\dot{p_2} = c_2 p_2 g(1 - p_1) - m_2 p_2 \tag{4.2}$$

$$\dot{p_3} = c_3 p_3 g(1 - p_1 - p_2) - m_3 p_3 \tag{4.3}$$

$$\dot{g} = -c_1 p_1 g - c_2 p_2 g(1 - p_1) - c_3 p_3 g(1 - p_1 - p_2) + m_1 p_1 + m_2 p_2 + m_3 p_3 \tag{4.4}$$

$$1 = p_1 + p_2 + p_3 + g, \tag{4.5}$$

where $\dot{}$ denotes $\frac{d}{dt}$.

We can see from equation (4.3) that species 3 can only colonise a vacant site if members of all species are absent. Again, equation (4.4) decouples from the system and using (4.5), we are left with:

$$\dot{p_1} = c_1 p_1 (1 - p_1 - p_2 - p_3) - m_1 p_1 \tag{4.6}$$

$$\dot{p_2} = c_2 p_2(1-p_1-p_2-p_3)(1-p_1) - m_2 p_2 \quad (4.7)$$

$$\dot{p_3} = c_3 p_3(1-p_1-p_2-p_3)(1-p_1-p_2) - m_3 p_3. \quad (4.8)$$

The equilibrium points (steady states) of the system are found from

$$\dot{p_1} = \dot{p_2} = \dot{p_3} = 0.$$

The eight possible steady states are given in Table (4.1), using the abbreviation $\gamma_i = \frac{m_i}{c_i}$ for $i = 1, 2, 3$.

state	p_1^0	p_2^0	p_3^0
(a)	0	0	0
(b)	0	0	$1-\gamma_3$
(c)	0	$1-\gamma_2$	0
(d)	$1-\gamma_1$	0	0
(e)	0	$1-\frac{\gamma_3}{\gamma_2}$	$\frac{\gamma_3}{\gamma_2}-\gamma_2$
(f)	$1-\frac{\gamma_3}{\gamma_1}$	0	$\frac{\gamma_3}{\gamma_1}-\gamma_1$
(g)	$1-\frac{\gamma_2}{\gamma_1}$	$1-\frac{\gamma_2}{\gamma_1}$	0
(h)	$1-\frac{\gamma_2}{\gamma_1}$	$\frac{\gamma_2}{\gamma_1}-\frac{\gamma_3}{\gamma_1}$	$\frac{\gamma_3}{\gamma_1}-\gamma_1$

Table 4.1: Steady states of (4.6) - (4.8)

The analysis from the two species model can be used to gain some insight into the three species model in each of the planes of the (p_1, p_2, p_3) space. The results of Chapter 3 may be extended here. For the steady states (a), and (e) to (g) we may apply the analysis of Chapter 3 as each of these steady states reduce to the two species case and are unstable to small perturbations. For steady states (b) to (d), the eigenvalues are considered in the following section.

There is only one steady state, (h), where all the species have a non-zero component. We are most interested in this steady state as we are aiming to model coexistence of species. The feasibility region for this in the $(\gamma_1, \gamma_2, \gamma_3)$ space is calculated from setting $1-\frac{\gamma_2}{\gamma_1} > 0$, $\frac{\gamma_2}{\gamma_1}-\frac{\gamma_3}{\gamma_1} > 0$ and $\frac{\gamma_3}{\gamma_1}-\gamma_1 > 0$. We find three inequalities:

$$\begin{aligned} \gamma_1 &> \gamma_2 \\ \gamma_2 &> \gamma_3 \\ \gamma_3 &\geq \gamma_1^2 \end{aligned}$$

which combined together to give us:

$$0 \leq \gamma_1^2 \leq \gamma_3 \leq \gamma_2 \leq \gamma_1 \leq 1. \quad (4.9)$$

Figure (4.1) shows the feasibility region in the planes of the parameter space for steady state (h) and Figure (4.2) shows the extension of the regions into the whole parameter space. The intersection of these planes and curves is the region in the parameter space where steady state (h) is feasible.

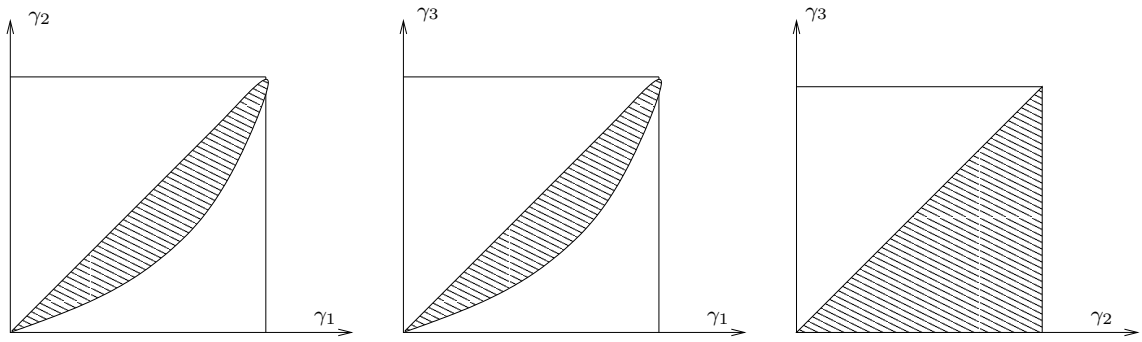


Figure 4.1: Feasibility regions for steady state (h) in the (γ_i, γ_j) planes

4.3 Preliminary Analysis

To perform linear stability analysis in three dimensions we must first consider the Jacobian matrix, **J**, where

$$(J)_{ij} = \frac{\partial \dot{p}_i}{\partial p_j}(p_1^0, p_2^0, p_3^0),$$

for $i, j = 1, 2, 3$.

Unfortunately the eigenvalues found from $\mid \mathbf{J} - \lambda \mathbf{I} \mid = 0 = d(\lambda)$ are even more complicated than in the two species case. For the steady states where at least two of the species have zero abundance I shall present the eigenvalues in Table (4.2), but for the remaining steady states (e)-(h) I shall leave the details to the Appendix. The eigenvalues for all steady states were calculated in Maple [6].

state	p_1^0	p_2^0	p_3^0	λ_1	λ_2	λ_3
(a)	0	0	0	$1-\gamma_1$	$1-\gamma_2$	$1-\gamma_3$
(b)	0	0	$1-\gamma_3$	$\gamma_3-\gamma_1$	$\gamma_3-\gamma_2$	$-1+\gamma_3$
(c)	0	$1-\gamma_2$	0	$\gamma_2-\gamma_1$	$-1+\gamma_2$	$\gamma_2^2-\gamma_3$
(d)	$1-\gamma_1$	0	0	$-1+\gamma_1$	$\gamma_1^2-\gamma_2$	$\gamma_1^2-\gamma_3$

Table 4.2: Steady states (a)-(d) and their associated eigenvalues from linear stability analysis

The eigenvalues for the steady state (h) involve so many terms that it is impossible to determine their sign by a simple method. We cannot employ surface plots as in Chapter 3

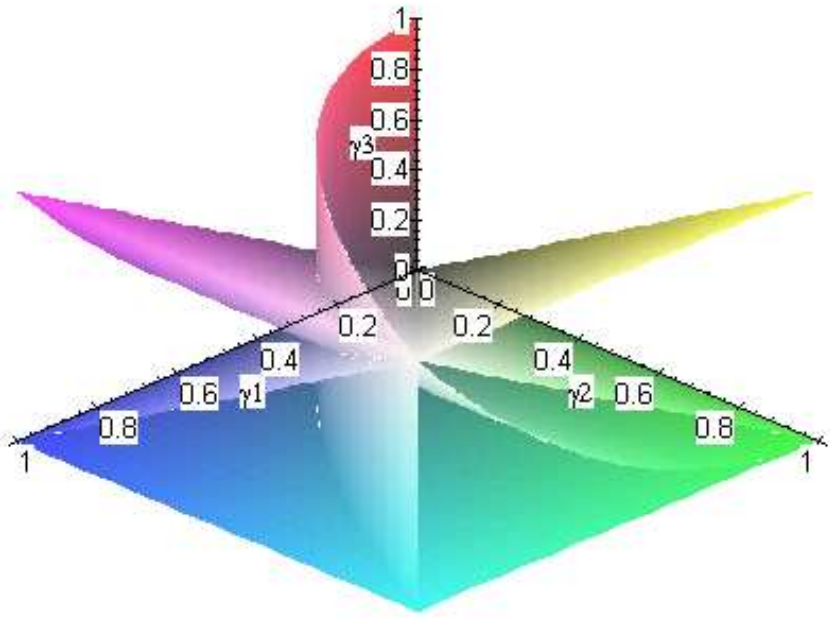


Figure 4.2: Feasibility regions for steady state (h) extended into the full 3-D parameter space

because we are now looking at eigenvalues as functions of three variables (γ_1, γ_2 and γ_3) and we would need four dimensions to view them.

4.4 Numerical Experiments

In order to gain some understanding of the likely behaviour in 3 dimensions, we began by conducting some numerical experiments. We carried out several numerical experiments for parameters within the feasibility region for steady state (h). For other regions of the parameter space the problem reduces to that for two species. The system is solved using MATLAB [15] `ode45`. An example of the results of our simulations are shown in Figure (4.3) and the parameter values and initial conditions used are given in Table (4.3). Each different coloured trajectory corresponds to a different initial condition, the dotted black lines correspond to nullclines in the $(p_i, p_j)-$plane, and the solid coloured lines correspond to trajectories. The dots correspond to unstable (red) and stable (green) steady states in the planes, with the magenta dot representing the steady state (h).

From our numerical experiments it seems that the steady state (h) with all species having a non-zero abundance is unstable. We have explored the parameter space extensively

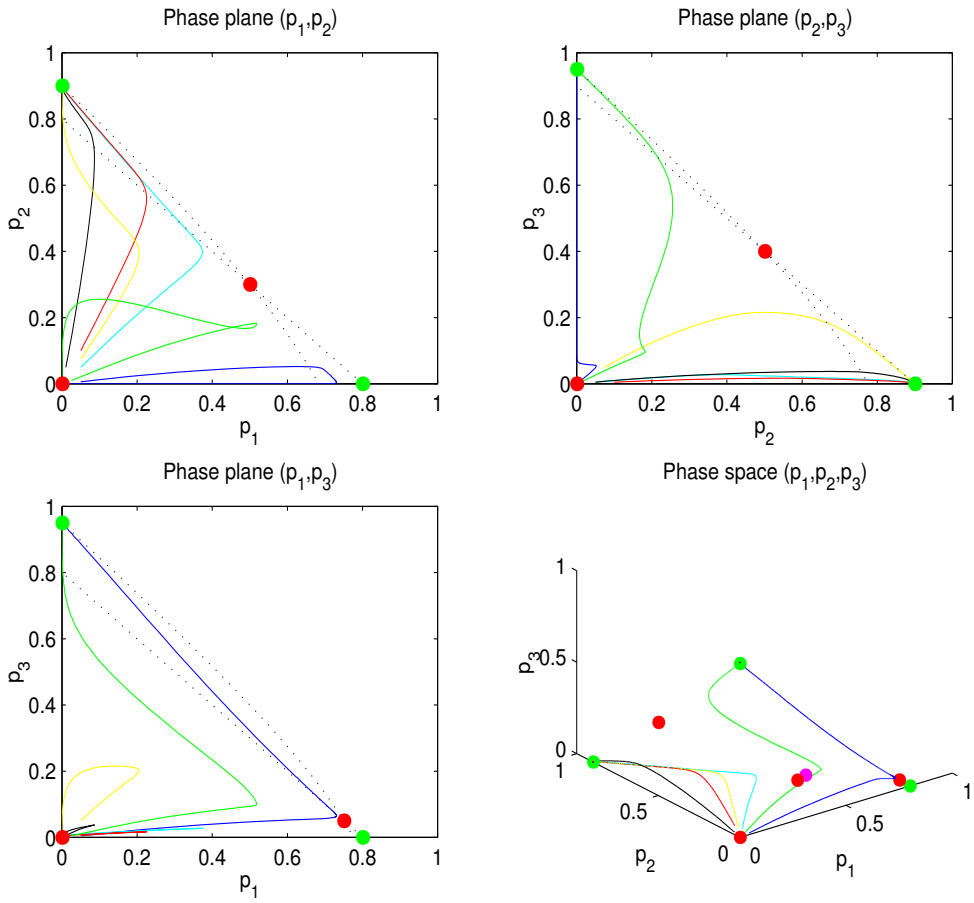


Figure 4.3: Phase planes and phase space for equations (4.6) - (4.8) for parameter values $\gamma_1 = 0.2$, $\gamma_2 = 0.1$, $\gamma_3 = 0.05$

and found no evidence to the contradict this hypothesis. Confirmation of this was given by considering the eigenvalues of each equilibrium point and showing numerically that at least one eigenvalue lies in the right half plane in each case.

A further experiment was completed taking an initial condition very close to the steady state (h). The results are shown in Figure (4.4), where the steady state (h) is depicted by a large black dot.

4.5 Further Stability Analysis

After the results of our numerical experiments we tried a different approach to determine the stability of the steady states of the system. We considered the form of the Jacobian matrix, **J**. We noticed from our numerical experiments that the Jacobian had the following

p_i	initial conditions/trajectory colours						
	blue	cyan	red	black	yellow	green	γ_i
p_1	0.050	0.050	0.050	0.010	0.050	0.025	0.20
p_2	0.006	0.050	0.100	0.050	0.075	0.010	0.10
p_3	0.005	0.005	0.005	0.005	0.050	0.005	0.05

Table 4.3: Initial conditions chosen for numerical simulations shown in Figure (4.3)

form in each case:

$$\mathbf{J} = \begin{pmatrix} a & a & a \\ \beta & b & b \\ \gamma & \gamma & c \end{pmatrix}. \tag{4.10}$$

We then performed some algebraic manipulation on the general form of $\mathbf{J}$ for case (h) and found that:

$$\begin{aligned} a &= -1 + \frac{\gamma_2}{\gamma_1} \\ b &= -\frac{\gamma_2}{\gamma_1}\left(\frac{\gamma_2}{\gamma_1} - \frac{\gamma_3}{\gamma_1}\right) \\ c &= -\frac{\gamma_3}{\gamma_1}\left(\frac{\gamma_3}{\gamma_1} - \gamma_1\right) \\ \beta &= -\left(\frac{\gamma_2}{\gamma_1} - \frac{\gamma_3}{\gamma_1}\right)\left(\frac{\gamma_2}{\gamma_1} + \gamma_1\right) \\ \gamma &= -\left(\frac{\gamma_3}{\gamma_1} - \gamma_1\right)\left(\frac{\gamma_3}{\gamma_1} + \gamma_1\right). \end{aligned}$$

In this simpler form it is then feasible to attempt to prove that one of the eigenvalues of the steady state (h) has a positive real part by considering the product of all the eigenvalues found from the determinant of the Jacobian. From $\mid \mathbf{J} - \lambda\mathbf{I} \mid = 0 = d(\lambda)$ we find that

$$\begin{aligned} d(\lambda) &= \lambda^3 - \lambda^2(a+b+c) + \lambda(ab+ac+bc+a\beta+a\gamma+b\gamma) - a(b-\beta)(c-\gamma) \\ &= \prod_{i=1}^{3}(\lambda - \lambda_i). \end{aligned} \tag{4.11}$$

Setting $\lambda = 0$, we find the product of the eigenvalues to be:

$$\prod_{i=1}^{3}\lambda_i = -a(b-\beta)(c-\gamma). \tag{4.12}$$

Now, using our inequality, (4.9), we have:

$$a < 0,$$

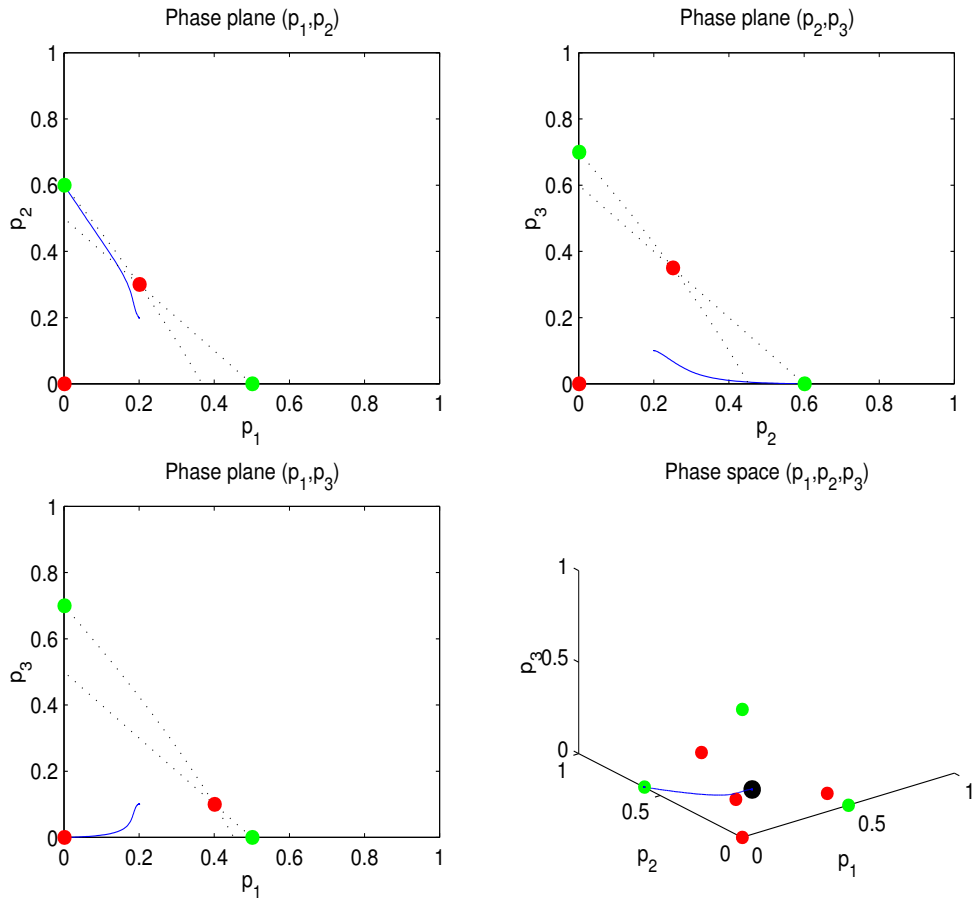


Figure 4.4: Phase planes and phase space for equations (4.6) - (4.8) for parameter values $\gamma_1 = 0.5$, $\gamma_2 = 0.4$, $\gamma_3 = 0.3$, initial conditions: $(p_1, p_2, p_3) = (0.200, 0.200, 0.100)$

$$b - \beta = \gamma_2 - \gamma_3 > 0$$

and

$$c - \gamma = \gamma_3 - \gamma_1^2 > 0.$$

Hence $\prod_{i=1}^{3} \lambda_i \geq 0$, and therefore there exists at least one eigenvalue, λ_i with $\mathbb{R}(\lambda_i) \geq 0$, hence the steady state (h) is unstable for all parameter values.

4.6 Conclusion

We have proved that this model (for three species) does not support a stable steady state with all three species coexisting. The general form of the Jacobian matrix, $\mathbf{J}$, will be investigated in the following chapter to determine whether the addition of more species allows a steady state with coexistence of all species to be stable. We will extend this analysis to n-species in the next chapter.

Chapter 5

n-Species Model

5.1 Introduction

We have shown in the previous two chapters that our model does not support stable coexistence of two or three species. We shall extend the analysis of Chapter 4 here to determine whether multiple species (> 3) coexistence can be stable.

5.2 Model and Determination of Steady States

Extending the model derived in Chapters 3 and 4 the system of non-linear ordinary differential equations becomes:

$$\dot{p_i} = c_i p_i g \left(1 - \sum_{j=1}^{i-1} p_j\right) - m_i p_i \tag{5.1}$$

$$\dot{g} = -\sum_{i=1}^{n} \left[c_i p_i g \left(1 - \sum_{j=1}^{i-1} p_j\right)\right] + \sum_{i=1}^{n} m_i p_i \tag{5.2}$$

$$1 = g + \sum_{i=1}^{n} p_i \tag{5.3}$$

for $i = 1, \ldots, n$.

The steady states are calculated in the same way as in the previous two chapters, setting the equations (5.1) to zero after using (5.3) to eliminate g. However, for our purposes, we are only interested in the steady state where all the species have a non-zero abundance, that is all species coexist, because the aim of our model is to predict long term coexistence of rainforest tree species. In this case the proportional abundances of the species are calculated to be:

$$p_1^0 = 1 - \frac{\gamma_2}{\gamma_1}$$

$$
\begin{aligned}
p_i^0 &= \frac{\gamma_i}{\gamma_1} - \frac{\gamma_{i+1}}{\gamma_1}, \text{for } \; i = 2, \ldots, n-1 \\
p_n^0 &= \frac{\gamma_n}{\gamma_1} - \gamma_1,
\end{aligned}
$$

where $\gamma_i = \frac{m_i}{c_i}$.

5.3 Stability Analysis

To find the general form of the Jacobian matrix, $\mathbf{J_n}$, we need to rewrite the system of equations (5.1) - (5.3), replacing $\frac{m_i}{c_i}$ by γ_i. We obtain the system:

$$
\frac{1}{c_i}\dot{p_i} = p_i \left(1 - \sum_{k=1}^{n} p_k\right)\left(1 - \sum_{k=1}^{i-1} p_k\right) - \gamma_i p_i, \tag{5.4}
$$

from which we find that:

$$
\begin{aligned}
\frac{1}{c_i}\frac{\partial \dot{p_i}}{\partial p_i} &= \left(1 - \sum_{k=1}^{n} p_k\right)\left(1 - \sum_{k=1}^{i-1} p_k\right) - p_i\left(1 - \sum_{k=1}^{i-1} p_k\right) - \gamma_i, && (5.5) \\
\frac{1}{c_i}\frac{\partial \dot{p_i}}{\partial p_j} &= -p_i\left(2 - \sum_{k=1}^{i-1} p_k - \sum_{k=1}^{n} p_k\right), \quad \text{for} \quad j < i, && (5.6) \\
\frac{1}{c_i}\frac{\partial \dot{p_i}}{\partial p_j} &= -p_i\left(1 - \sum_{k=1}^{i-1} p_k\right), \quad \text{for} \; \; j > i. && (5.7)
\end{aligned}
$$

Considering first the case $i = 1$, in (5.4), we obtain $p_1 = 0$ or $1 - \sum_{i=1}^{n} p_i = \gamma_1$. Substituting this into Equation (5.4) for $i \geq 2$, we see that $1 - \sum_{k=1}^{i-1} p_k = \frac{\gamma_i}{\gamma_1}$. Substituting this into equations (5.5) - (5.7), the entries of the Jacobian become:

$$
\begin{aligned}
\frac{\partial \dot{p_i}}{\partial p_j} &= -p_i\left(\frac{\gamma_i}{\gamma_1} + \gamma_1\right), \quad \text{for} \; \; j < i, && (5.8) \\
\frac{\partial \dot{p_i}}{\partial p_j} &= -p_i\frac{\gamma_i}{\gamma_1}, \quad \text{for} \; \; j \geq i. && (5.9)
\end{aligned}
$$

The general Jacobian matrix, $\mathbf{J_n}$ is:

$$
\mathbf{J_n} = \begin{pmatrix}
-p_1 & -p_1 & \cdots & \cdots \\
-p_2\left(\frac{\gamma_2}{\gamma_1} + \gamma_1\right) & -p_2\frac{\gamma_2}{\gamma_1} & -p_2\frac{\gamma_2}{\gamma_1} & \cdots \\
-p_3\left(\frac{\gamma_3}{\gamma_1} + \gamma_1\right) & -p_3\left(\frac{\gamma_3}{\gamma_1} + \gamma_1\right) & -p_3\frac{\gamma_3}{\gamma_1} & \cdots \\
\vdots & \vdots & \ddots & \ddots \\
-p_n\left(\frac{\gamma_n}{\gamma_1} + \gamma_1\right) & \vdots & \ddots & -p_n\frac{\gamma_n}{\gamma_1}
\end{pmatrix} = \begin{pmatrix}
a_1 & a_1 & a_1 & \cdots \\
\alpha_2 & a_2 & a_2 & \cdots \\
\alpha_3 & \alpha_3 & a_3 & \cdots \\
\vdots & \vdots & \ddots & \ddots \\
\alpha_n & \vdots & \ddots & a_n
\end{pmatrix}. \tag{5.10}
$$

We will use the following theorem and corollary in our stability analysis.

Theorem 5.1 *$\exists$ at least one eigenvalue of the stability matrix, $\mathbf{J_n}$, in the right half of the complex plane.*

Corollary 5.1 *The system of equations (5.4) for $n > 1$ has only at most one possible stable steady state. This is the steady state in which only one of the species is non-zero and all the other species die out.*

Proof 5.1 (of Theorem 5.1) *We know $p_i \geq 0$ and $0 \leq \gamma_1^2 \leq \gamma_n \leq \ldots \leq \gamma_2 \leq \gamma_1 \leq 1$, hence we have that $a_1 < 0$, and $a_i - \alpha_i \geq 0 \quad \forall i$. The LU decomposition of $\mathbf{J_n}$ is:*

$$\mathbf{LU} = \begin{pmatrix} 1 & 0 & \ldots & \ldots \\ \frac{\alpha_2}{a_1} & 1 & 0 & \ldots \\ \frac{\alpha_3}{a_1} & 0 & 1 & 0 \\ \vdots & \vdots & \ddots & \ddots \\ \frac{\alpha_n}{a_1} & \vdots & \ddots & 1 \end{pmatrix} \begin{pmatrix} a_1 & a_1 & \ldots & \ldots \\ 0 & a_2 - \alpha_2 & a_2 & \ldots \\ 0 & 0 & a_3 - \alpha_3 & \ldots \\ \vdots & \vdots & \ddots & \ddots \\ 0 & \vdots & \ddots & a_n - \alpha_n \end{pmatrix}.$$

To calculate the eigenvalues of the system, we need to look at $\mid \mathbf{J_n} - \lambda \mathbf{I} \mid = \prod_{i=1}^{n} (\lambda - \lambda_i)$. Setting $\lambda = 0$ we have $\mid \mathbf{J_n} \mid = (-1)^n \prod_{i=1}^{n} \lambda_i$. From the LU decomposition of $\mathbf{J_n}$ we know that

$$\mid \mathbf{J_n} \mid = a_1(a_2 - \alpha_2)(a_3 - \alpha_3) \ldots (a_n - \alpha_n) < 0.$$

For n even we have $\prod_{i=1}^{n} \lambda_i < 0$ and for n odd, we have $\prod_{i=1}^{n} \lambda_i > 0$ (since $a_1 < 0$ and $a_i - \alpha_i > 0 \quad \forall i$). In either case there is always at least one eigenvalue with $\mathbb{R}(\lambda_i) > 0$.

Proof 5.2 (of Corollary 5.1) *From Theorem 5.1 we know that the steady state with all n-species having a non-zero abundance is unstable. Hence the system reduces to that of $(n-1)$-species. Similarly this reduces by one dimension, until we are left with a 2-species system. In Chapter 3 we have shown that the only stable steady state is for one species dominating and the other decaying to zero. In the 1-species case, the only possible stable steady state is for $p_1 = 1 - \frac{m_1}{c_1} > 0$. The steady state $(p_1, 0, \ldots, 0)$ for n-species is stable since all its eigenvalues, which can be easily shown to be $\lambda_1 = -1 + \gamma_1, \quad \lambda_i = \gamma_1^2 - \gamma_i \quad i = 2, \ldots, n$, are less than zero since $\gamma_i > \gamma_1^2 \quad \forall i$.*

5.4 Conclusion

We have proved that our model does not mimic the long term coexistence and diversity observed in the tropical rainforests. We need to consider another mechanism for simulating this species richness. A new approach is discussed in Chapter 6, that is the inclusion of fruiting events and non-constant colonisation rates.

Chapter 6

Fruiting Events

6.1 Motivation for Model

The model described in Chapters 3 - 5 does not support the stable coexistence of species. We have proved that in the absence of random fruiting events and seedling abundance decay we cannot achieve long-term co-existence and diversity. Therefore in order to test our hypothesis (Chapter 1), we introduce random fruiting events. It is not possible to do any analysis on such a complex system, instead we investigate the parameter space by numerical simulation.

6.2 Description of Model

6.2.1 Colonisation Rates

The number of seedlings of any particular species decays with time over the course of a fruiting cycle. Data collected indicates that this decay is exponential and thus we take the colonisation rates to be of the following form:

$$c_i = \alpha_i e^{-\beta_i t} \tag{6.1}$$

where β_i is the decay rate of seedlings of species i per year. The new meaning of c_i is that it is the *absolute colonisation power* of species i, that is the ability of a seedling of species i to "win" a site given that the species has been recruited to a site. α_i is the initial value of the colonisation power for species i at the start of every fruiting cycle.

6.2.2 Model Dynamics Equations

Our new model for n species then becomes:

$$\dot{p_i} = (\alpha_i e^{-\beta_i t}) p_i g \left(1 - \sum_{j=1}^{i-1} p_j\right) - m_i p_i \tag{6.2}$$

$$\dot{g} = -\sum_{i=1}^{n} \left[(\alpha_i e^{-\beta_i t}) p_i g \left(1 - \sum_{j=1}^{i-1} p_j\right)\right] + \sum_{i=1}^{n} m_i p_i \tag{6.3}$$

$$1 = g + \sum_{i=1}^{n} p_i \tag{6.4}$$

for $i = 1, ..., n$, or, eliminating g,

$$\dot{p_i} = (\alpha_i e^{-\beta_i t}) p_i \left(1 - \sum_{j=1}^{n} p_j\right) \left(1 - \sum_{j=1}^{i-1} p_j\right) - m_i p_i. \tag{6.5}$$

This is solved over the length of a fruiting interval.

6.3 Problems with determination of parameter values

Unfortunately, there is very little experimental data available to indicate the appropriate values for our colonisation parameters (c_i, α_i, and β_i, see below for definitions) and to a lesser extent, the mortality rates (m_i). We have contacted David Tilman [29] to see if he could provide any insight. He explained that he first explored his model (equations (2.6)) theoretically to determine the plausibility of a colonisation-competition mechanism to explain coexistence. From this he determined the necessary relationships among parameters for coexistence. He then set the colonisation ability of the dominant species and explored the general phenomenon, using data on competitive abilities and seed production rates to estimate the parameters. His parameter values led to a predicted successional dynamics and coexistence that seemed to qualitatively mimic the patterns seen in his grasslands.

Based on Tilman's reply, we decided the most appropriate approach is to attempt to find the range of parameters by numerical simulation, based on experimental values that are available. Therefore we determined by some simple analysis, comparing the magnitude of proliferation (c_i, α_i, β_i) and the decay (m_i) parameters, the likely range of each parameter based on the experimental data available. We then explored this space numerically to determine the effects of each of the parameters, and more particularly, whether any set of parameters could give long-term coexistence for large numbers of species in the presence of random fruiting events. The results are presented in section 6.4, first for six species,

species	α_i	β_i	$\bar{c}_i$	m_i	γ_i	initial conditions
p_1	0.2883	0.8047	0.0510	0.0255	0.50	0.1603
p_2	0.3254	0.8179	0.0566	0.0255	0.45	0.1603
p_3	0.3933	0.8796	0.0638	0.0255	0.40	0.1603
p_4	0.4670	0.9144	0.0728	0.0255	0.35	0.1603
p_5	0.6707	1.1647	0.0823	0.0255	0.31	0.1603
p_6	0.8092	1.2239	0.0944	0.0255	0.27	0.1603

Table 6.1: Parameter values and initial conditions for numerical experiments displayed in Figure (6.1)

then for two, four and 180 species. The way in which we determined the possible ranges of parameters is discussed in detail in Appendix C.

6.4 Numerical Experiments

Our system, equations (6.5), is solved over the length of a fruiting interval. The fruiting interval is a random amount of time after which the seedling bank is replenished and the c_i $(i = 1, \ldots, n)$ are reset to their initial values, taking the current values of $(p_1, \ldots, p_n)$ as the new initial conditions in order to solve the system.

A uniform random number generator provides the time between fruiting events in our simulations with the mean, t_f, and variance taken from data supplied by Dr. Nick Brown (a discussion into the time distribution of fruiting events is to be found in Appendix C.6). The system of non-linear equations are solved using MATLAB [15] `ode15s` (an implicit, multi-step numerical ODE solver of varying order (1-5)).

Data for six species was collected and numerical experiments carried out based on this data to determine whether our model predicts the dynamics of tree species observed in the rainforest. Figure (6.1) shows the results. Sub-plot (1) shows a simulation with random fruiting events and decaying colonisation powers. Sub-plot (2) is included for comparison, to demonstrate that the fruiting events and the decaying parameters allow coexistence of many species. The parameter values and initial conditions are given in Table (6.1).

In Figure (6.1) it can be seen that all the proportional abundances of the species drop before any of them begin to increase. This indicates that the parameter values obtained from the data are not necessarily very accurate.

We shall now return to the two species case to see if parameter values can be calculated that enable coexistence in the fruiting model and then build up the number of species from

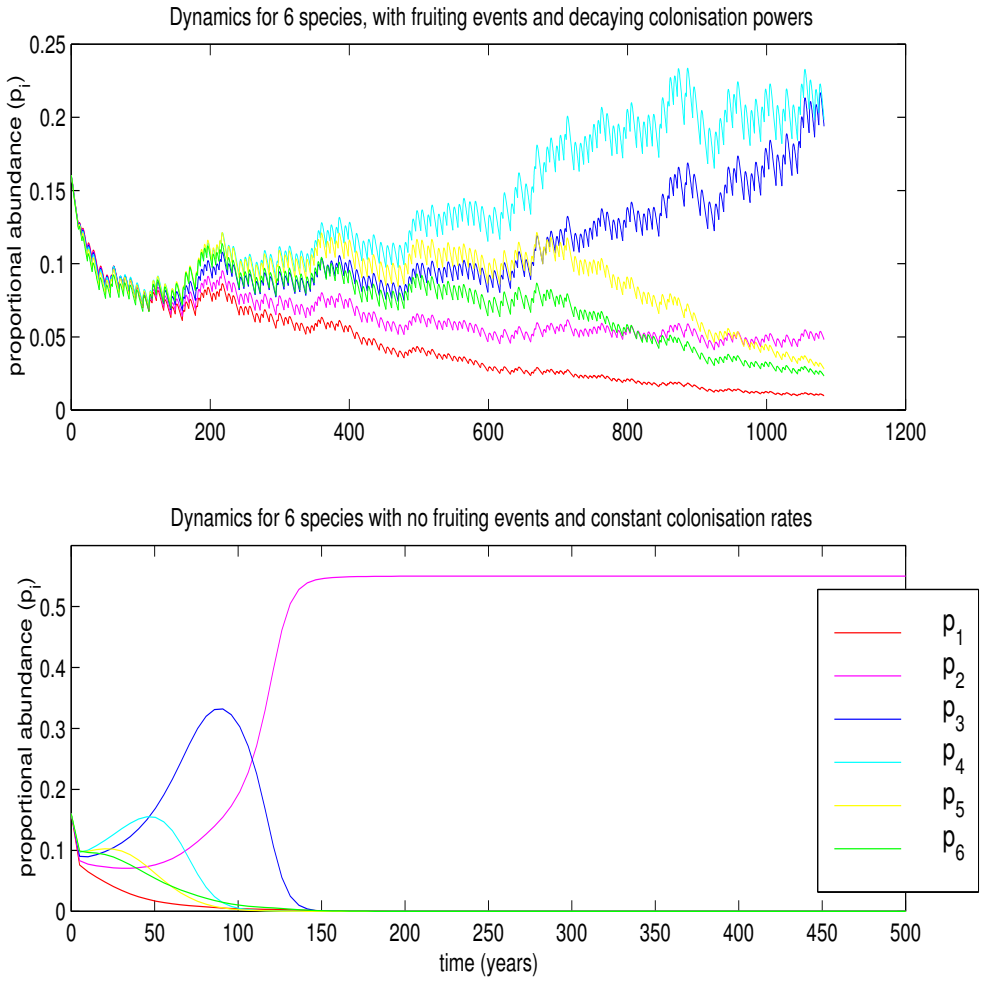


Figure 6.1: Dynamics of competition, equation (6.2) - (6.4) between 6 species. The top panel includes fruiting and decaying c_i, while the bottom panel shows that the simulation run without fruiting events and constant c_i results in one species dominating, after less than 150 years.

there. Details of determination of the parameters are described in Appendix C (particularly C.7).

Figure (6.2) shows the results with the parameter values given in Table (6.2). We can see that small changes in parameter values can cause very different dynamics. In sub-plot (1) we have both species switching over in abundance, and both are present in approximately the same proportions after 500 years. In sub-plots (2) and (3), slight changes in the parameters have caused one of the species to totally dominate the other.

Extending the experiments for 2 species we now present results for 4 species in Figure (6.3). It can be seen that the dynamics of the species are very sensitive to slight changes in parameters from the data given in Table (6.3). However, very different parameter values

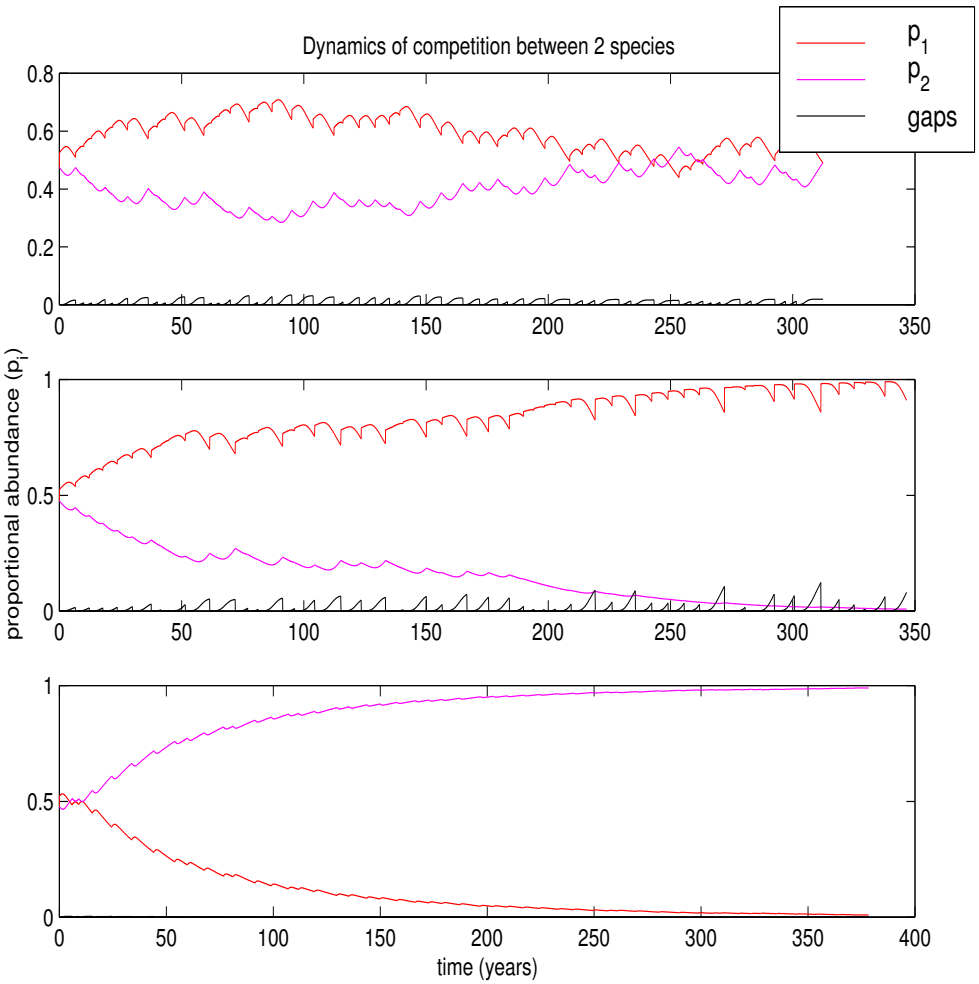


Figure 6.2: Dynamics of competition between 2 species, for the model (6.2) - (6.4), in sub-plot(1), both species are present after 350 years, but in sub-plots (2) and (3) one species is seen to dominate the other

were required in order for all the species to co-exist over time.

In practice there are 180 species in an average hectare of the rainforest. We need to determine whether our model can qualitatively reproduce the dynamics observed in the rainforest. To this aim, we have conducted some numerical experiments.

The results of simulations for 180 species, are shown in Figures (6.4) and (6.5). Only every 20th species is shown in each plot. Because the system is so sensitive to changes in parameters, the simulation in Figure (6.5) does not show all species switching over in abundance order or having a similar abundance at the end of the simulation. However, the proportional abundance of gaps (about 4%) is approximately the value observed in practice. In Figure (6.5) all competitors have a final proportional abundance between 0.0023 and 0.0028, however the proportion of gap (about 50%) is much larger than the observed value

Sub-plot	**species**	α_i	β_i	m_i	initial conditions
(1)	p_1	500	1.6	0.0255	0.475
	p_2	9	0.05	0.0255	0.475
(2)	p_1	550	1.2	0.0255	0.475
	p_2	9	0.05	0.0255	0.475
(3)	p_1	350	2.0	0.0255	0.475
	p_2	35	0.05	0.0255	0.475

Table 6.2: Parameter values and initial conditions for experiments displayed in Figure (6.2)

Sub-plot	**species**	α_i	β_i	m_i	initial conditions
(1)	p_1	425	1.8	0.0255	0.2375
	p_2	275	1.25	0.0255	0.2375
	p_3	10	0.131	0.0255	0.2375
	p_4	9.5	7.5×10^{-8}	0.0255	0.2375
(2)	p_1	425	1.8	0.0255	0.2375
	p_2	275	1.3	0.0255	0.2375
	p_3	10	0.11	0.0255	0.2375
	p_4	9.5	1×10^{-7}	0.0255	0.2375
(3)	p_1	425	1.8	0.0255	0.2375
	p_2	275	1.1	0.0255	0.2375
	p_3	10	0.12	0.0255	0.2375
	p_4	9.5	1×10^{-7}	0.0255	0.2375
(4)	p_1	475	1.6	0.0255	0.2375
	p_2	275	1.2	0.0255	0.2375
	p_3	10	0.12	0.0255	0.2375
	p_4	9.5	1×10^{-7}	0.0255	0.2375

Table 6.3: Parameter values and initial conditions for experiments displayed in Figure (6.3)

(about 3%), however the species are all seen to switch over in the dominance hierarchy. The parameter sets used are given in Tables (6.4) and (6.5).

6.5 Potential Adaptation to Model

The above model, equations (6.5), appears to be very sensitive to changes in parameters. From this we proposed that the competitive rank of the species might change during a fruiting interval. In order to incorporate this into our model the following adaptation was made:

$$\dot{p_i} = (\alpha_i e^{-\beta_i t}) p_i g \left(1 - \sum_{j=1}^{i-1} e^{-\beta_j t} p_j\right) - m_i p_i. \tag{6.6}$$

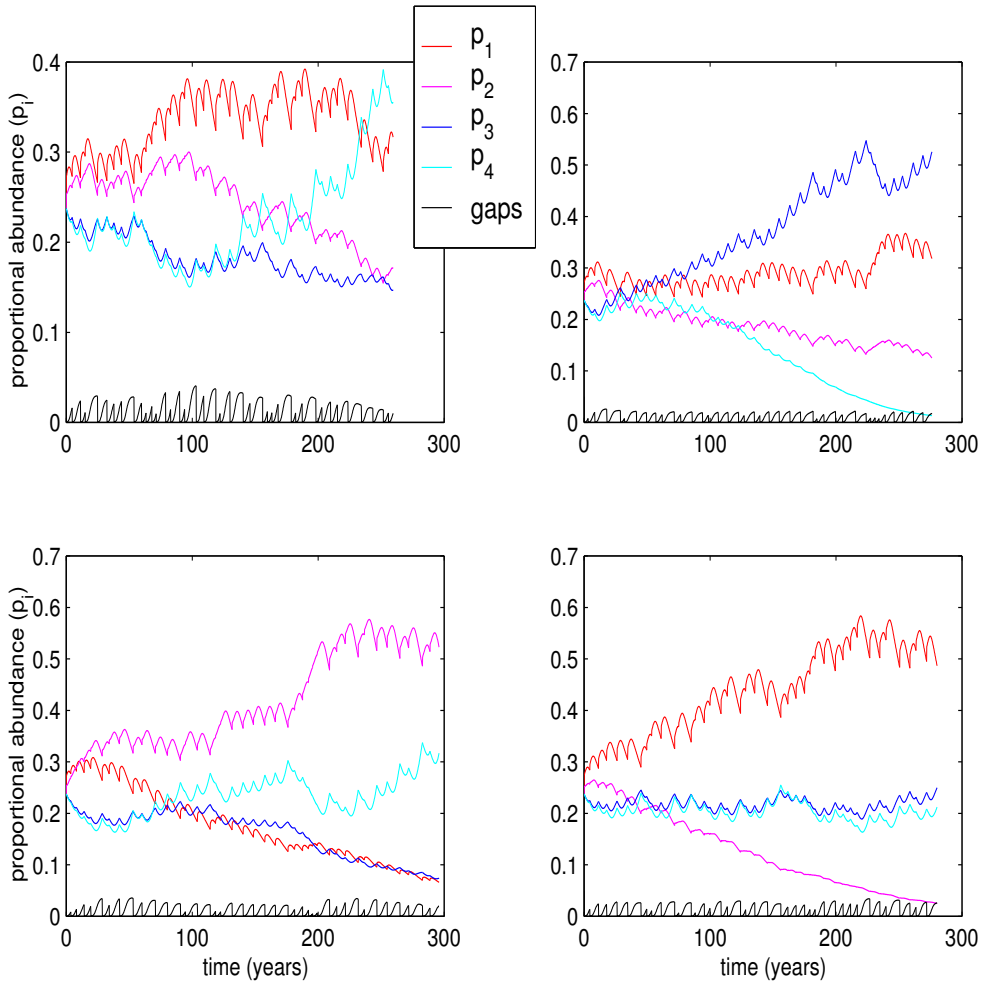


Figure 6.3: Dynamics of competition between 4 species, for the model (6.2) - (6.4), in sub-plot(1), all species are present after 350 years, but in sub-plots (2), (3) and (4) one or more of the species are seen to start to die out.

In this way, the effect of competition on the system declines over a fruiting interval. Similar results were obtained to the previous model (without the adaptation). A simulation for two species is given in Figure (6.6). The parameter values used are shown in Table (6.6). This model is less sensitive to changes in parameter values.

6.6 Conclusion

From our numerical experiments we can infer that the inclusion of random fruiting events into our model has enabled us to reproduce the kind of dynamics that are observed in the rainforest. Species are seen to coexist over much longer periods of time (1000 years) than was seen for our earlier model (150 years to single species taking over), by which time

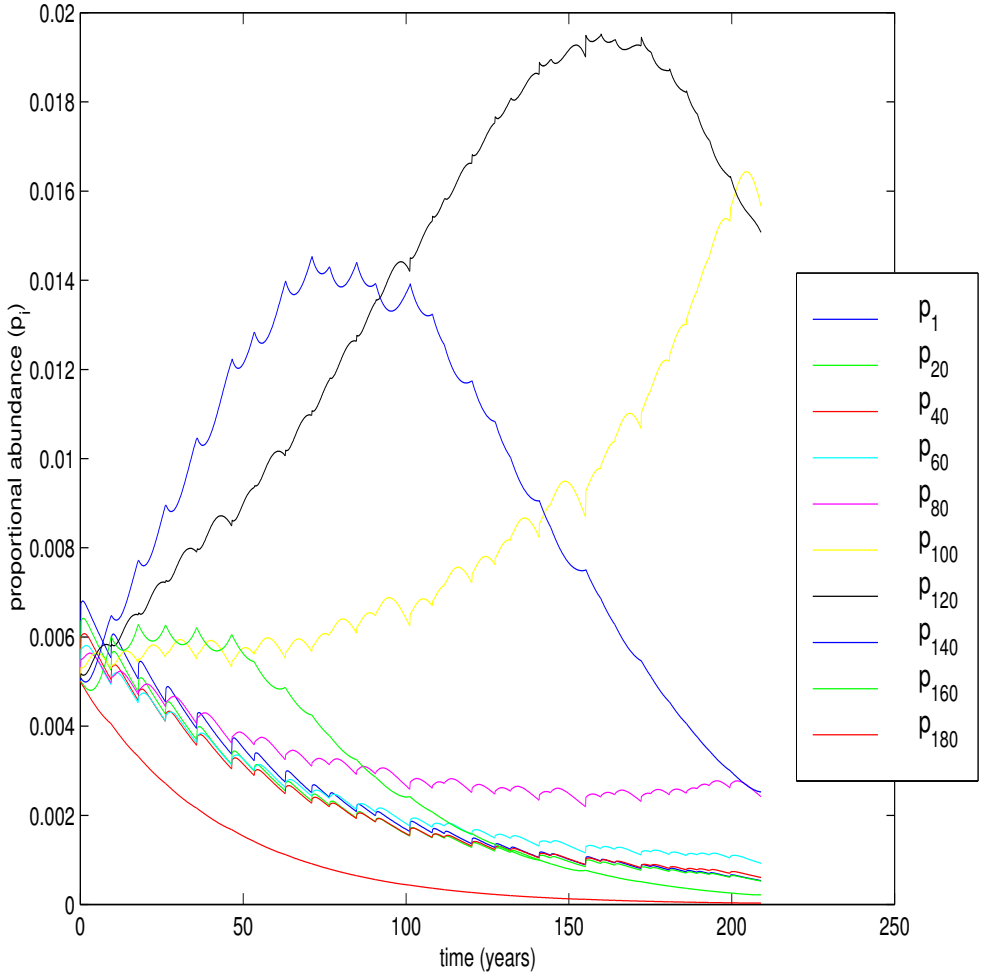


Figure 6.4: Dynamics of competition between 180 species, for the model (6.2) - (6.4). See text for details.

more genetic mutations will have occurred and the dynamics altered in another way.

Although our model including seedling population decay and random fruiting events does allow greater diversity over time, the parameter values that we have been forced to use are unrealistic compared to those derived from data and given in Table (6.1). If we use the parameter values in Table (6.1), then we obtain a very large gap proportion, caused by the downward pressure on each species due to competition. This suggests that the diversity seen in rainforests is not due to competition at all, and we discuss a very simple model in the next chapter which will allow the diversity seen in real rainforests.

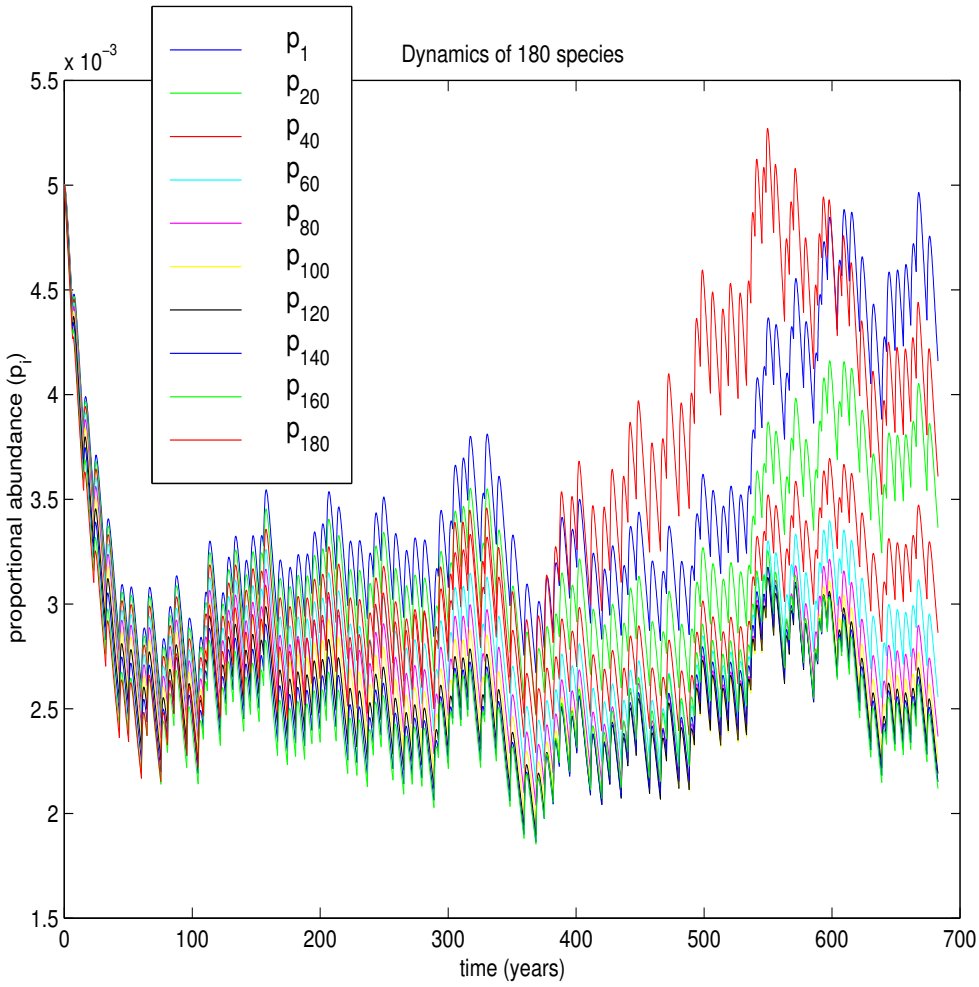


Figure 6.5: Dynamics of competition between 180 species, for the model (6.2) - (6.4), showing that all species are present after 700 years

species	α_i	β_i	m_i	init. cond.
p_1	450	3.1343	0.0255	0.005
p_i $(i = 2, 116)$	450 $-2.4301(i-1)$	$\frac{\alpha_i}{7.1785}(0.05 - 2.5 \times 10^{-4}(i-1))$	0.0255	0.005
p_i $(i = 117, 149)$	450 $-2.4301(i-1)$	$\frac{\alpha_i}{7.1785}(0.05 - 2.5 \times 10^{-4}(i-1))$ $+0.035$	0.0255	0.005
p_i $(i = 150, 180)$	450 $-2.4301(i-1)$	$\frac{\alpha_i}{7.1785}(0.05 - 2.5 \times 10^{-4}(i-1))$ -0.0005	0.0255	0.005

Table 6.4: Parameter values and initial conditions for experiments displayed in Figure (6.4)

species	α_i	β_i	$\bar{c}_i$	m_i	γ_i	initial cond.
p_1	0.2883	0.8047	0.0510	0.0255	0.50	0.005
p_i $(i = 2, 179)$	$\frac{\beta_i t_f \bar{c}_i}{1-e^{-\beta_i t_f}}$	0.8047 $+(i-1)0.0023$	$\frac{m_i}{\gamma_i}$	0.0255	0.5 $-(i-1)0.0013$	0.005
p_n	0.8397	1.2239	0.0980	0.0255	0.26	0.005

Table 6.5: Parameter values and initial conditions for experiments displayed in Figure (6.5)

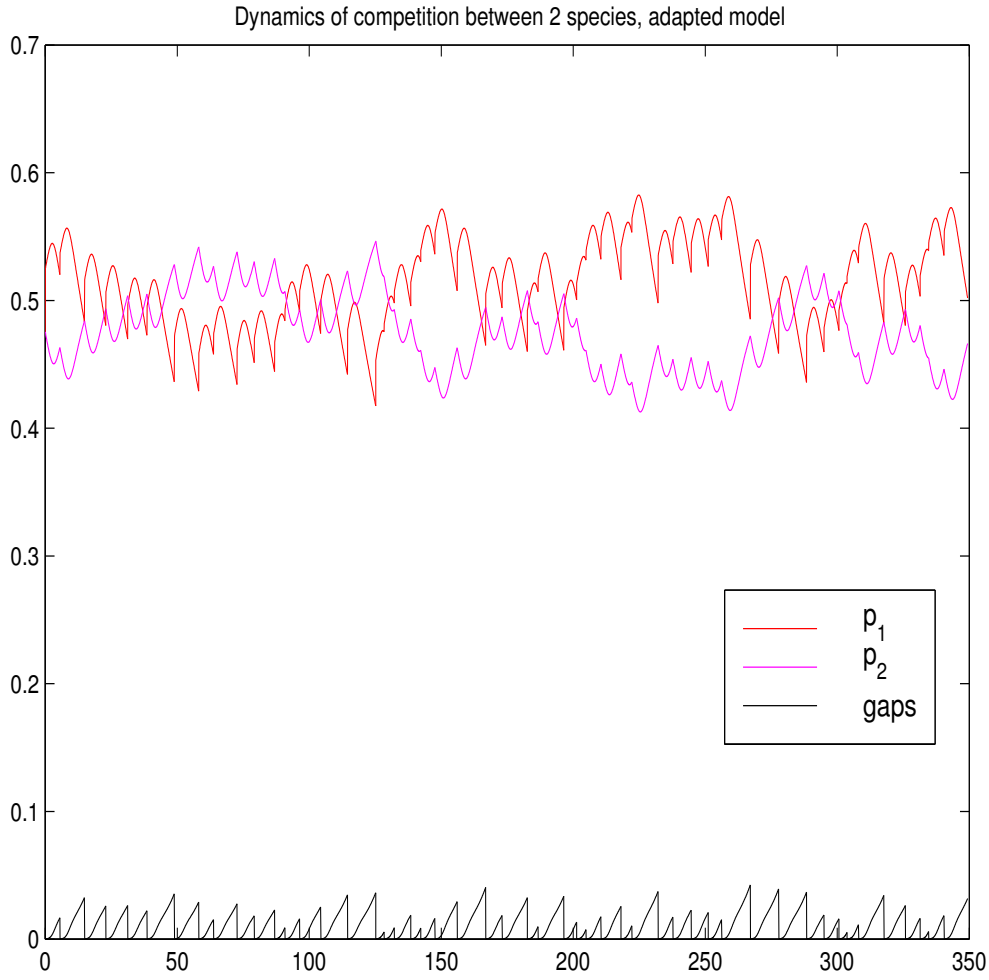


Figure 6.6: Dynamics of competition between 2 species, with an adaptation of the model to (6.6)

species	α_i	β_i	m_i	initial conditions
p_1	500	1.6	0.0255	0.475
p_2	9	0.2	0.0255	0.475

Table 6.6: Parameter values and initial conditions for experiments displayed in Figure (6.6)

Chapter 7

No Competition

7.1 Description of Model

Returning to our original model given in equations (5.1) - (5.3), we can remove competition between species altogether by removing the $\left(1 - \sum_{j=1}^{i-1} p_j\right)$ term in (5.2). The system of equations then becomes:

$$\dot{p}_i = c_i p_i g - m_i p_i \tag{7.1}$$

$$\dot{g} = -\sum_{i=1}^{n} c_i p_i g + \sum_{i=1}^{n} m_i p_i \tag{7.2}$$

$$1 = g + \sum_{i=1}^{n} p_i. \tag{7.3}$$

Again, g decouples and we obtain:

$$\dot{p}_i = c_i p_i \left(1 - \sum_{i=1}^{n} p_i\right) - m_i p_i. \tag{7.4}$$

Assuming that $c_i = c = constant, \quad \forall i$ and $m_i = m = constant, \quad \forall i$ and setting $P = \Sigma p_i$, and summing equation (7.4) over n, we see that:

$$\dot{P} = cP(1 - P) - mP, \tag{7.5}$$

which is equivalent to Tilman's [28] model for one species and has a stable steady state at $P = 1 - \frac{m}{c}$. With $m = 0.01$, we can set $c = 0.3$ and obtain the correct gap, and co-existence of all species. Seedling decay can then be introduced using the actual observed values, and the results are shown in Figure (7.1) for six trees. The parameter values used are shown in Table (7.1).

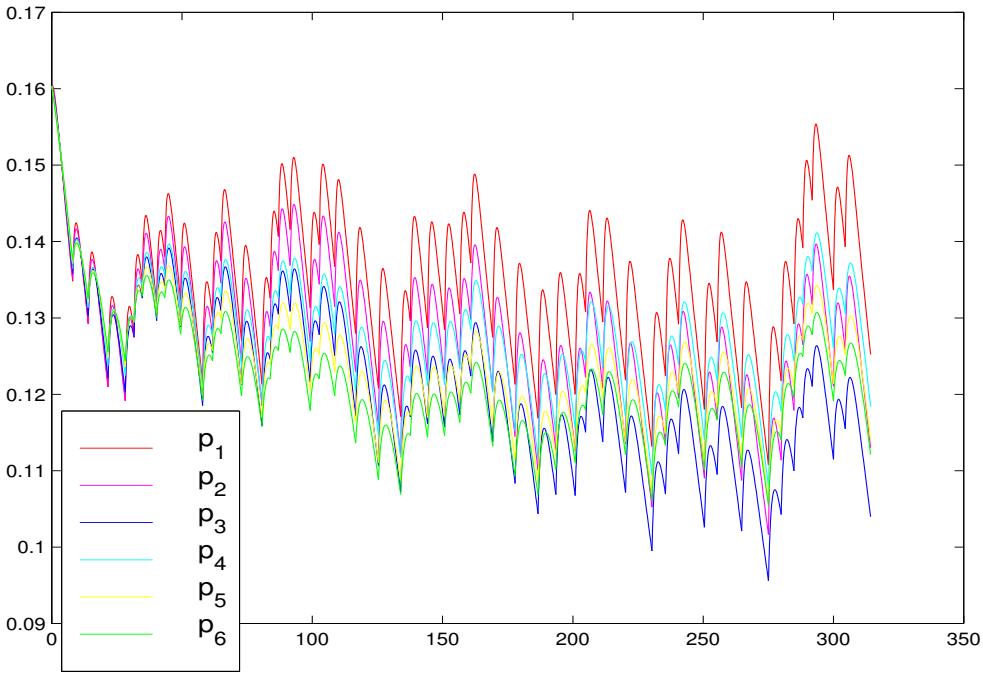


Figure 7.1: Dynamics of competition between 6 species, with no competition.

species	α_i	β_i	m_i	initial conditions
p_1	0.8092	1.2239	0.0255	0.1603
p_2	0.6707	1.0147	0.0255	0.1603
p_3	0.4670	0.6894	0.0255	0.1603
p_4	0.3933	0.5546	0.0255	0.1603
p_5	0.3254	0.4429	0.0255	0.1603
p_6	0.2883	0.3797	0.0255	0.1603

Table 7.1: Parameter values and initial conditions for experiments displayed in Figure (7.1)

7.2 Conclusion

We have developed a simple model with no competition, which leads to the sort of diversity seen in the rainforest. This result supports the hypothesis of rainforest diversity held by Hubbell [17].

Chapter 8

Conclusion

8.1 Plausibility of Hypothesis

In Chapters 3 to 5 we have proved that for species coexistence it is not enough for the colonisation rates of each species to remain constant, and in Chapter 6 we have demonstrated that long term coexistence is possible with the inclusion of random fruiting events and decaying colonisation powers.

We have shown that competition between species cannot lead to the type of species diversity observed in real rainforests using realistic parameter values. We have therefore developed a simple model, with *no* competition, and incorporated Brown's hypothesis in the role of seedling population decay. We have shown in Chapter 7 that this simpler model can account for diversity over time with realistic parameter values.

In this dissertation we have shown that Brown's hypothesis (Chapter 1) that random mass fruiting events and the differing abilities of species to persist, as seedlings, after these events is a plausible mechanism for maintaining high diversity in the Borneo rainforest.

8.2 Areas of Further Work

There are many possible areas of further modelling. Some of the models presented in Chapter 2 have implications in modelling tropical rainforests.

We would like to carry out further work into a model without any competition between the different species, incorporating an age structured model, starting from that described by Clark & Ji [7], and could include the dynamics of seedlings (young), saplings (adolescents) and adults of different tree species.

Habitat destruction (by human intervention), for example, is a major area of concern for ecologists and the models of Tilman *et al* [30] amongst others will provide a clue as to how to extend our model. In addition to this, we also could include random stochastic

events, such as landslides and forest fires, both of which are natural occurrences that affect the composition of the forest afterwards.

Further investigation of the stochastic models including those due to Hurtt & Pacala [18] may yield a more accurate model.

A major area of further work, that we have not even touched upon, is spatial variation. There are many papers that describe this kind of work and many directly cite Tilman's model [28]. The extension of our model to a system of partial differential equations would enable us to predict the behaviour of tree species in different areas of the forest and how they interact with each other over space, not just time.

We also need to determine whether our model, equation (6.5), is sufficient to describe the dynamics of competition, or whether we need an adaptation similar to that proposed in Section 6.5.

Appendix A

Parameter Definitions

symbol	definition
α_i	initial colonisation power of species i
β_i	seedling decay rate of species i
c_i	colonisation power of species i
$\bar{c_i}$	average colonisation power over fruiting interval
$d(\lambda)$	$\mid \mathbf{J} - \lambda \mathbf{I} \mid$
γ_i	$\frac{m_i}{c_i}$ (Chapters 3 - 5 only)
g	proportion of free space (gaps)
$\mathbf{J}$ ($\mathbf{J_n}$)	Jacobian matrix (for n species)
λ_i	eigenvalues
m_i	mortality rate of species i
n	number of species
p_i	proportional abundance of species i
p_i^0	steady value of p_i
$\widetilde{p_i}$	small perturbation of p_i^0
t	time
t_f	average fruiting cycle length

Table A.1: Parameter Symbols and Definitions

Appendix B

Eigenvalues for Three Species Model

For the three species model (4.6) - (4.8), the eigenvalues that determine linear stability and steady states with less than two species having zero abundance were calculated using Maple [6] and are displayed in the following Table (B.1).

state	p_1^0	p_2^0	p_3^0	λ_1	λ_2	λ_3
(e)	0	$1-\frac{\gamma_3}{\gamma_2}$	$\frac{\gamma_3}{\gamma_2}-\gamma_2$	$\hat{\lambda_1}^{(e)}$	$\hat{\lambda_2}^{(e)}$	$\hat{\lambda_3}^{(e)}$
(f)	$1-\frac{\gamma_3}{\gamma_1}$	0	$\frac{\gamma_3}{\gamma_1}-\gamma_1$	$\hat{\lambda_1}^{(f)}$	$\hat{\lambda_2}^{(f)}$	$\hat{\lambda_3}^{(f)}$
(g)	$1-\frac{\gamma_2}{\gamma_1}$	$1-\frac{\gamma_2}{\gamma_1}$	0	$\hat{\lambda_1}^{(g)}$	$\hat{\lambda_2}^{(g)}$	$\hat{\lambda_3}^{(g)}$
(h)	$1-\frac{\gamma_2}{\gamma_1}$	$\frac{\gamma_2}{\gamma_1}-\frac{\gamma_3}{\gamma_1}$	$\frac{\gamma_3}{\gamma_1}-\gamma_1$	$\hat{\lambda_1}^{(h)}$	$\hat{\lambda_2}^{(h)}$	$\hat{\lambda_3}^{(h)}$

Table B.1: steady states

where:

$$
\begin{aligned}
\hat{\lambda_1}^{(e)} &= \gamma_2-\gamma_1 \\
\hat{\lambda_2}^{(e)} &= \frac{1}{2\gamma_2^2}(-\gamma_2^2+\gamma_2\gamma_2-\gamma_3^2+\gamma_3\gamma_2^2 \\
&\quad +\sqrt{}(\gamma_2^4-2\gamma_3\gamma_2^3+3\gamma_3^2\gamma_2^2+2\gamma_2^4\gamma_3-2\gamma_3^3\gamma_2-2\gamma_3^2\gamma_2^3+\gamma_3^4-2\gamma_3^3\gamma_2^2+\gamma_3^2\gamma_2^4 \\
&\quad +4\gamma_2^5\gamma_3-4\gamma_2^6)) \\
\hat{\lambda_3}^{(e)} &= \frac{1}{2\gamma_2^2}(-\gamma_2^2+\gamma_2\gamma_2-\gamma_3^2+\gamma_3\gamma_2^2 \\
&\quad -\sqrt{}(\gamma_2^4-2\gamma_3\gamma_2^3+3\gamma_3^2\gamma_2^2+2\gamma_2^4\gamma_3-2\gamma_3^3\gamma_2-2\gamma_3^2\gamma_2^3+\gamma_3^4-2\gamma_3^3\gamma_2^2+\gamma_3^2\gamma_2^4 \\
&\quad +4\gamma_2^5\gamma_3-4\gamma_2^6)) \\
\hat{\lambda_1}^{(f)} &= \gamma_3-\gamma_3 \\
\hat{\lambda_2}^{(f)} &= \frac{1}{2\gamma_1^2}(-\gamma_1^2+\gamma_3\gamma_1-\gamma_3^2+\gamma_3\gamma_1^2 \\
&\quad +\sqrt{}(\gamma_1^4-2\gamma_3\gamma_1^3+3\gamma_3^2\gamma_1^2+2\gamma_1^4\gamma_3-2\gamma_3^3\gamma_1-2\gamma_3^2\gamma_1^3+\gamma_3^4-2\gamma_3^3\gamma_1^2+\gamma_3^2\gamma_1^4
\end{aligned}
$$

$$
\begin{aligned}
& +4\gamma_1^5\gamma_3 - 4\gamma_1^6)) \\
\hat{\lambda_3}^{(f)} &= \frac{1}{2\gamma_1^2}(-\gamma_1^2 + \gamma_3\gamma_1 - \gamma_3^2 + \gamma_3\gamma_1^2 \\
& -\sqrt{(\gamma_1^4 - 2\gamma_3\gamma_1^3 + 3\gamma_3^2\gamma_1^2 + 2\gamma_1^4\gamma_3 - 2\gamma_3^3\gamma_1 - 2\gamma_3^2\gamma_1^3 + \gamma_3^4 - 2\gamma_3^3\gamma_1^2 + \gamma_3^2\gamma_1^4} \\
& +4\gamma_1^5\gamma_3 - 4\gamma_1^6)) \\
\hat{\lambda_1}^{(g)} &= \gamma_1^2 - \gamma_3 \\
\hat{\lambda_2}^{(g)} &= \frac{1}{2\gamma_1^2}(-\gamma_1^2 + \gamma_2\gamma_1 - \gamma_2^2 + \gamma_2\gamma_1^2 \\
& +\sqrt{(\gamma_1^4 - 2\gamma_2\gamma_1^3 + 3\gamma_2^2\gamma_1^2 + 2\gamma_1^4\gamma_2 - 2\gamma_2^3\gamma_1 - 2\gamma_2^2\gamma_1^3 + \gamma_2^4 - 2\gamma_2^3\gamma_1^2 + \gamma_2^2\gamma_1^4} \\
& +4\gamma_1^5\gamma_2 - 4\gamma_1^6)) \\
\hat{\lambda_3}^{(g)} &= \frac{1}{2\gamma_1^2}(-\gamma_1^2 + \gamma_2\gamma_1 - \gamma_2^2 + \gamma_2\gamma_1^2 \\
& -\sqrt{(\gamma_1^4 - 2\gamma_2\gamma_1^3 + 3\gamma_2^2\gamma_1^2 + 2\gamma_1^4\gamma_2 - 2\gamma_2^3\gamma_1 - 2\gamma_2^2\gamma_1^3 + \gamma_2^4 - 2\gamma_2^3\gamma_1^2 + \gamma_2^2\gamma_1^4} \\
& +4\gamma_1^5\gamma_2 - 4\gamma_1^6)) \\
\hat{\lambda_1}^{(h)} &= \sqrt[3]{\Gamma_1} - \frac{1}{9}\Gamma_2 + \frac{1}{3}\Gamma_3 \\
\hat{\lambda_2}^{(h)} &= -\frac{1}{2}\sqrt[3]{\Gamma_1} + \frac{1}{18}\Gamma_2 + \frac{1}{3}\Gamma_3 + \frac{1}{2}i\sqrt{2}\left(\sqrt[3]{\Gamma_1} + \frac{1}{9}\Gamma_2\right) \\
\hat{\lambda_3}^{(h)} &= -\frac{1}{2}\sqrt[3]{\Gamma_1} + \frac{1}{18}\Gamma_2 + \frac{1}{3}\Gamma_3 - \frac{1}{2}i\sqrt{2}\left(\sqrt[3]{\Gamma_1} + \frac{1}{9}\Gamma_2\right)
\end{aligned}
$$

where Γ_1 is a polynomial approximately 40 lines long,

$$
\begin{aligned}
\Gamma_2 &= \frac{1}{\gamma_1^4\sqrt[3]{\Gamma_1}}(2\gamma_2\gamma_1^2\gamma_3 - 2\gamma_2\gamma_1^3\gamma_3 - 3\gamma_2\gamma_1^4\gamma_3 + 2\gamma_2\gamma_3^3 - \gamma_3^4 - 2\gamma_1\gamma_3\gamma_2^2 + 2\gamma_1\gamma_2\gamma_3^2 \\
& -\gamma_2^2\gamma_3\gamma_1^2 + \gamma_2\gamma_3^2\gamma_1^2 + 2\gamma_3\gamma_2^3 - 3\gamma_3^2\gamma_2^2 - \gamma_2^4 - 2\gamma_3^2\gamma_1^2 + 2\gamma_1^4\gamma_3 + 2\gamma_3^3\gamma_1^2 - \gamma_3^2\gamma_1^4 \\
& -\gamma_1^4 + 3\gamma_1^6 + 2\gamma_2\gamma_1^3 - 3\gamma_2^2\gamma_1^2 - 3\gamma_1^4\gamma_2 + 2\gamma_2^3\gamma_1 + 3\gamma_2^2\gamma_1^3 + 3\gamma_2^2\gamma_1^4 - 3\gamma_1^5\gamma_2)
\end{aligned}
$$

and

$$
\Gamma_3 = \frac{1}{\gamma_1^2}(-\gamma_2^2 + \gamma_2\gamma_3 - \gamma_3^2 + \gamma_3\gamma_1^2 + \gamma_2\gamma_1 - \gamma_1^2).
$$

Appendix C

Derivation of Parameters

C.1 Decay Rates (β_i)

The rate of decay of the seedlings for each species can be extrapolated from the time course data from field work. Figure (C.1) shows the time course of seedling data for 9 species. For the first three species data comes from tropical lowland forest at Danum Valley, Sabah, Peninsular Malaysia by Whitmore & Brown [31]. For the remaining 6 species, data is taken from the Sandakan Forest Reserve by Fox [12]. For the last 6 species, only 2 data points were available. Since the β_i we calculated from the slope of the plots, any small change in either of the data points would lead to a big difference in the value of β_i calculated.

C.2 Colonisation Rates (α_i)

From our analysis of the previous model (5.1) - (5.3), we found regions in the parameter space where coexistence is feasible (but unstable for the model with constant colonisation rates). This feasibility region is given as:

$$0 \leq \gamma_1^2 \leq \gamma_n \leq \gamma_{n-1} \leq ... \leq \gamma_2 \leq \gamma_1 \leq 1,$$

where γ_i is now defined to be $\gamma_i = \frac{m_i}{\bar{c_i}}$ and $\bar{c_i}$ is the average value of c_i over the fruiting interval. i.e.

$$\bar{c_i} = \frac{1}{t_f} \int_0^{t_f} \alpha_i e^{-\beta_i t} \mathrm{d}t, \tag{C.1}$$

and t_f is the average length of a fruiting cycle. In this way, taking a certain parameter set for $(\gamma_1, ..., \gamma_n)$ and given values for $(m_1, ..., m_n)$ we can calculate $(\bar{c_1}, ..., \bar{c_n})$ and then from the formulae in (C.1) we can calculate $(\alpha_1, ..., \alpha_n)$ given $(\beta_1, ..., \beta_n)$.

The definition of $\bar{c_i}$ enables us to run experiments without fruiting events which may be compared directly to those with fruiting events. This parameter also gives us the competitive ordering of species, with $\bar{c_1}$ being the smallest.

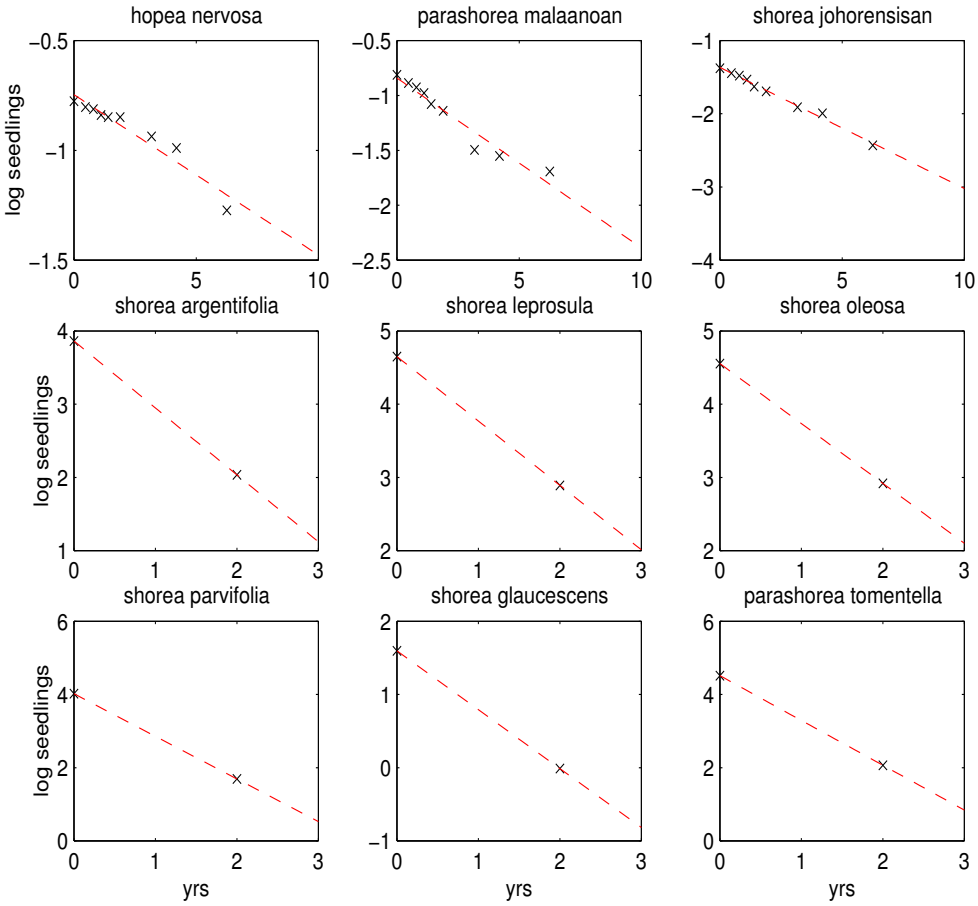


Figure C.1: Time course of seedlings on forest floor

C.3 Mortality Rates (m_i)

No accurate values for mortality rates have been collected for individual species, due to small sample plots and the relatively small time-scale of data collection. The minimum is given as 1.4% per annum and the maximum is 3.7% per annum, corresponding to a tree life-span of 71.4 years and 27.0 years respectively (data taken from tropical lowland forest at Danum Valley, Sabah, Peninsular Malaysia). As no accurate values are known, in general, an average mortality rate is used for all species based on the minimum and maximum recorded values for all species in the tropical rainforest.

C.4 Initial Proportional Abundances

In an average hectare (10,000 m^2) in the rainforest there are approximately 180 species which occupy 96% of the space. There is approximately 4% of free space (gap). This means that each species on average has a proportional abundance of 0.005. When less than

180 species are modelled, the gap proportion is kept the same and the initial proportional abundances of the species is calculated by dividing up equally the remaining space.

C.5 Ratios of Mortality to Colonisation

We also found that the ratios $c_i : m_i$ at $t = 0$ and $m_i : c_i$ at $t = t_f$ are of a similar order of magnitude for all species (from data taken from the Sandakan Forest Reserve by Fox [12]). This indicates that at some point during a fruiting interval the colonisation terms balance the mortality terms in equation (6.2). It is expected to be the case that a species is as many times more likely to colonise immediately after a fruiting event as it is to die immediately before a fruiting event. In calculating the c_i there has to be a balance between proliferation and death, if the death component is too large then the species will die out.

C.6 Fruiting Interval Length and Distribution

The observed length of time between fruiting events is between three and eleven years. We shall take the average to be seven years and taken from a uniform distribution.

The distribution of the fruiting events is thought to follow the distribution of El Niño episodes [32]. General flowering regions coincide with areas with low night-time temperatures about two months before flowering. It is thought that low air temperature induces the development of floral buds of the Dipterocarpaceae. Low night-time temperatures usually occur in La Niña episodes (following El Niño episodes). We have taken the distribution of fruiting events to be uniformly distributed. However some experiments have been carried out with a normal distribution, but we obtain similar results.

C.7 Balance of Proliferation and Death of Species

Finally we decided to determine, as a guide, the ratio of $\alpha_i : \beta_i$ demanding that the proportions of each species should return to its initial proportion after an average fruiting interval, t_f. Assuming that p_i and g are constant (as there are only small changes in proportions), we then find for the two species model:

$$\int_0^{t_f} p_1 \mathrm{d}t = p_1 g \alpha_1 \int_0^{t_f} e^{-\beta_1 t} \mathrm{d}t - p_1 m_1 \int_0^{t_f} \mathrm{d}t \tag{C.2}$$

For $p_1 \neq 0$ we obtain:

$$\frac{\alpha_1}{\beta_1} = \frac{(1 + m_1) t_f}{g} \tag{C.3}$$

and similarly for species 2:

$$\frac{\alpha_2}{\beta_2} = \frac{(1+m_2)t_f}{g(1-p_1)}. \tag{C.4}$$

For the ith species, the ratio of α_i to β_i is given by:

$$\frac{\alpha_i}{\beta_i} = \frac{(1+m_i)t_f}{g(1-\sum_{j=1}^{i-1} p_j)}. \tag{C.5}$$

These expressions are used as a starting point to find the parameter values.

References

[1] P. S. ASHTON. *Dynamics of tropical communities*, chapter Niche specificity among tropical trees: a question of scales. D. M. Newbery, H. H. T. Prins and N. D. Brown editors. Oxford: Blackwell Science, 1998.

[2] JOHN E. BANKS. Do imperfect trade-offs affect the extinction debt phenomenon? *Ecology*, **78**:1597–1601, 1997.

[3] SEBASTIAN BONHOEFFER, ROBERT M. MAY, GEORGE M. SHAW, AND MARTIN A. NOWAK. Virus dynamics and drug therapy. *Proceedings of The National Academy of Sciences (USA), Medical Sciences*, **94**:6971–6976, 1997.

[4] N. V. L. BROKAW AND S. M. SCHEINER. Species composition in gaps and structure of a tropical forest. *Ecology*, **70**:538–541, 1989.

[5] NICK D. BROWN, M. PRESS, AND D. BEBBER. Growth and survivorship of dipterocarp seedlings: differences in shade persistence create a special case of dispersal limitation. *Philosophical Transactions of the Royal Society of London, Series B (Biological Sciences)*, **354**, in press.

[6] BRUCE W. CHAR, KEITH O. GEDDES, GASTON H. GONNET, BENTON L. LEONG, MICHAEL B. MONAGAN, AND STEPHEN M. WATT. *Maple V, version 5, Language Reference Manual*. Waterloo Maple Software, 1991.

[7] JAMES S. CLARK AND YUAN JI. Fecundity and dispersal in plant populations: implications for structure and diversity. *The American Naturalist*, **146**:72–111, 1995.

[8] R. F. COSTANTINO, J. M. CUSHING, BRIAN DENNIS, AND R. A. DESHARNAIS. Experimentally-induced transitions in the dynamic behaviour of insect populations. *Nature*, **375**:227–230, 1995.

[9] R. F. COSTANTINO, J. M. CUSHING, BRIAN DENNIS, R. A. DESHARNAIS, AND S. M. HENSON. Resonant population cycles in temporally fluctuating habitats. *Bulletin of Mathematical Biology*, **60**:247–273, 1998.

[10] R. F. COSTANTINO, R. A. DESHARNAIS, J. M. CUSHING, AND BRIAN DENNIS. Chaotic dynamics in an insect population. *Science*, **275**:389–391, 1997.

[11] BRIAN DENNIS, R. A. DESHARNAIS, J. M. CUSHING, AND R. F. COSTANTINO. Non-linear demographic dynamics - mathematical models, statistical methods, and biological experiments. *Ecological Monographs*, **65**:261–281, 1995.

[12] J. E. D. FOX. *The natural vegetation of Sabah and natural regeneration of the dipterocarp forests.* PhD thesis, University of Wales, 1972.

[13] L. GOLDWASSER, J. COOK, AND E. D. SILVERMAN. The effects of variability on metapopulation dynamics and rates of invasion. *Ecology*, **75**:40–47, 1994.

[14] P. J. GRUBB. The maintenance of species richness in plant communities: the importance of the regeneration niche. *Biological Review*, **52**:107–145, 1977.

[15] DUANE HANSELMAN AND BRUCE LITTLEFIELD. *Mastering* MATLAB*, A comprehensive tutorial and reference.* The MathWorks, Inc., 1996.

[16] S. M. HENSON AND J. M. CUSHING. The effect of periodic habitat fluctuations on a non-linear insect population model. *Journal of Mathematical Biology*, **36**:201–226, 1997.

[17] S. P. HUBBELL. Tree dispersion, abundance, and diversity in a tropical dry forest. *Science*, **203**:1299–1309, 1979.

[18] GEORGE C. HURTT AND STEPHEN W. PACALA. The consequences of recruitment limitation: reconciling chance, history and competitive differences between plants. *Journal of Theoretical Biology*, **176**:1–12, 1995.

[19] GEORGE P. MALANSON. Effects of dispersal and mortality on diversity in a forest stand model. *Ecological Modelling*, **87**:103–110, 1996.

[20] ROBERT M. MAY AND MARTIN A. NOWAK. Superinfection, metapopulation dynamics, and the evolution of diversity. *Journal of Theoretical Biology*, **170**:95–114, 1994.

[21] R. DANIEL MORTON AND RICHARD LAW. Regional species pools and the assembly of local ecological communities. *Journal of Theoretical Biology*, **187**:321–331, 1997.

[22] J. MOSQUERA AND FREDERICK R. ADLER. Evolution of virulence: a unified framework for co-infection and superinfection. *Journal of Theoretical Biology*, **195**:293–313, 1998.

[23] STEPHEN W. PACALA AND MARK REES. Models suggesting field experiments to test two hypotheses explaining successional diversity. *The American Naturalist*, **152**:729–737, 1998.

[24] ALAN S. PERELSON, PAULINA ESSUNGER, YUNZHEN CAO, MIKA VESANEN, ARLENE HURLEY, KALLE SAKSELA, MARTIN MARKOWITZ, AND DAVID D. HO. Decay characteristics of HIV-1 infected compartments during combination therapy. *Nature*, **387**:188–191, 1997.

[25] GRAEME D. RUXTON AND MICHAEL DOEBELI. Spatial self-organisation and perisistence of transients in a metapopulation model. *Proceedings of the Royal Society of London, Series B - Biological Sciences*, **263**:1153–1158, 1996.

[26] N. I. STILIANAKIS, C. A. B. BOUCHER, M. D. DEJONG, R. VANLEEUWEN, R. SCHUURMAN, AND R. J. DEBOER. Clinical data sets of human immunodeficiency virus type 1 reverse transcriptase-resistant mutant explained by a mathematical model. *Journal of Virology*, **71**:161–168, 1997.

[27] LEWI STONE AND SMADAR EZRATI. Chaos, cycles and spatiotemporal dynamics in plant ecology. *Journal of Ecology*, **84**:279–291, 1996.

[28] DAVID TILMAN. Competition and biodiversity in spatially structured habitats. *Ecology*, **75**:2–16, 1994.

[29] DAVID TILMAN. Colonisation coefficients. Personal communication, August 1999.

[30] DAVID TILMAN, ROBERT M. MAY, CLARENCE M. LEHMAN, AND MARTIN A. NOWAK. Habitat destruction and the extinction debt. *Nature*, **371**:65–66, 1994.

[31] T. C. WHITMORE AND NICK D. BROWN. Dipterocarp seedling growth in rain forest canopy gaps during six and a half years. *Philosophical Transactions of the Royal Society of London, Series B (Biological Sciences)*, **351**:1195–1203, 1996.

[32] MASATOSHI YASUDA, JUN MATSUMOTO, NORIYUKI OSADA, SAN'EI ICHIKAWA, AKIO FURUKAWA, ABDUL RAHIM NIK, AND N. MANOKARAN. The mechanism of general flowering in Dipterocarpaceae in the Malay Peninsula. *Journal of Tropical Ecology*, **15**:437–449, 1999.

[33] DOUGLAS W. YU, JOHN W. TERBOROUGH, AND MATTHEW D. POTTS. Can high species richness be explained by Hubbell's null model? *Ecology Letters*, **1**:193–199, 1998.

[34] DA-YONG ZHANG AND I. HANSKI. Sexual reproduction and stable coexistence of identical competitors. *Journal of Theoretical Biology*, **193**:465–473, 1998.

[35] DA-YONG ZHANG AND KUI LIN. The effects of competitive asymmetry on the rate of competitive displacement: how robust is Hubbell's community drift model? *Journal of Theoretical Biology*, **188**:361–367, 1997.